NASA TECHNICAL MEMORANDUM

NASA TM X-1240

NASA TM X-1240

SUMMARY OF PRELIMINARY DATA DERIVED FROM THE XB-70 AIRPLANES

by William H. Andrews

Flight Research Center
Edwards, Calif.

NATIONAL AERONAUTICS AND SPACE ADMINISTRATION • WASHINGTON, D. C. • JUNE 1966

NASA TM X-1240

SUMMARY OF PRELIMINARY DATA DERIVED FROM THE XB-70 AIRPLANES

By William H. Andrews

NASA Flight Research Center
Edwards, Calif.

NATIONAL AERONAUTICS AND SPACE ADMINISTRATION

For sale by the Clearinghouse for Federal Scientific and Technical Information
Springfield, Virginia 22151 – Price $2.00

SUMMARY OF PRELIMINARY DATA

DERIVED FROM THE XB-70 AIRPLANES*

By William H. Andrews
Flight Research Center

SUMMARY

Preliminary data obtained during the initial flight-envelope expansion of the XB-70 airplanes are presented in the areas of stability and control, general performance, propulsion-system inlet operation, structural thermal response, internal noise, runway noise, and sonic boom.

The general handling qualities and performance of the airplane over the flight envelope appeared to be satisfactory; however, excessive longitudinal elevon trim and associated adverse aileron yaw characteristics were noted, particularly in the transonic speed range. Landing approach speeds were between 40 and 50 knots higher than those of current jet transports, and sink rates at touchdown were within the range of 1 to 4 feet per second experienced by the transports. Preliminary analysis indicates that the airplane experiences a measurable increase in lift near the ground plane; however, additional testing is required to define the magnitude of the increased lift.

Initial propulsion-system inlet operations were conservative, and a sacrifice of 5 to 10 percent in pressure recovery below a normal inlet operational range was accepted during maneuvering flights at the higher Mach numbers. Near-optimum inlet-pressure recovery was obtained prior to inlet "unstart" conditions with the airplane held in stabilized level flight.

Structural temperature measurements compared well with predictions. Dense structures, such as the wing-fold actuators, indicated an appreciable lag in response to the thermal gradients.

In the transition from subsonic to supersonic speed, the internal noise levels were reduced approximately 10 decibels between Mach numbers of 0.80 and 1.2; in the supersonic range, the cockpit noise level was comparable to that of current jet transports in cruise flight. Preliminary noise levels measured for an average slant range from the microphones of 750 feet during takeoff and 540 feet during landing were 138 decibels and 110 decibels, respectively.

Sonic-boom data indicated that near-field effects, measured on the ground, may be experienced at higher aircraft operational altitudes than anticipated.

---

*This paper was presented in the NASA Flight Research Center Special Projects Review on October 8, 1965, at Edwards, Calif. The data presented are representative of those available on that date.

INTRODUCTION

Within the limited inventory of operational high-performance aircraft, the XB-70 airplane incorporates unique features of configuration, systems, propulsion, and performance that are conducive to generalized flight research applicable to the design of future airplanes of this type. Thus, the National Aeronautics and Space Administration is conducting a series of investigations of flight dynamics, performance and propulsion, loads, and environmental factors (see table I) utilizing data generated during the flight testing of the airplane. Because of the nature of the current test program, i.e., envelope expansion and vehicle and systems demonstration, only limited data have been obtained in these areas in conjunction with the flight testing of the prototype airplanes. References 1 and 2 report some of the data acquired during the early flights in the program. This paper amplifies the earlier summary reports and presents more recent data accumulated during the expansion of the flight envelope. The data were obtained under the conditions normally experienced in an initial airplane demonstration program and, thus, should be treated as preliminary. As such, they are not conducive to final analysis.

SYMBOLS

b	wing span, feet
C_l	rolling-moment coefficient, $\frac{\text{Rolling moment}}{qSb}$
C_{l_β}	effective dihedral parameter, $\frac{\partial C_l}{\partial \beta}$, per degree
$C_{l_{\delta_a}}$	aileron-effectiveness parameter, $\frac{\partial C_l}{\partial \delta_a}$, per degree
C_m	pitching-moment coefficient, $\frac{\text{Pitching moment}}{qS\bar{c}}$
C_{m_α}	static longitudinal-stability parameter, $\frac{\partial C_m}{\partial \alpha}$, per degree
C_{m_δ}	equivalent longitudinal-control effectiveness, $\frac{\partial C_m}{\partial \delta}$, per degree
C_{m_o}	pitching-moment coefficient at zero lift, $\frac{M_o}{qS\bar{c}}$
C_n	yawing-moment coefficient, $\frac{\text{Yawing moment}}{qSb}$
C_{n_β}	static directional-stability parameter, $\frac{\partial C_n}{\partial \beta}$, per degree

$C_{n_{\delta_a}}$	variation of yawing moment with aileron deflection, $\frac{\partial C_n}{\partial \delta_a}$, per degree
$\bar{c}$	wing mean aerodynamic chord, feet
h_p	pressure altitude, feet
Δh	geometric altitude above the sonic-boom measuring site, feet
M	Mach number
M_o	pitching moment at zero lift, foot-pound
q	dynamic pressure, $\frac{1}{2}\rho V^2$, pounds per square foot
$\left(p_{t_2}\right)_{av}$	average of the total pressures measured at the engine-compressor faces (left-hand duct), pounds per square inch
p_{t_∞}	free-stream total pressure calculated from nose-boom pitot measurement, pounds per square inch
Δp	incremental sonic-boom overpressure, pounds per square foot
S	wing area, square feet
V	velocity, feet per second
α	angle of attack, degrees
β	angle of sideslip, degrees
δ	equivalent longitudinal-control deflection, degrees
δ_a	aileron deflection, degrees
ρ	density of air, slugs per cubic foot

TEST AIRPLANES

The XB-70 was designed as a long-range, supersonic-cruise airplane capable of flying at an approximate sustained speed of Mach 3 and an altitude of 70,000 feet. Two airplanes were built and designated the XB-70-1 and the XB-70-2. Figure 1 is a three-view drawing of the XB-70-1 airplane. Pertinent physical characteristics of the airplanes are presented in table II. The basic design incorporates a thin, low-aspect-ratio, 65.6° sweptback leading-edge, delta-wing with folding tips, twin vertical stabilizers, and a movable canard with trailing-edge flaps. The propulsion package includes a two-dimensional, mixed-compression, twin-inlet system which houses six engines in

the aft portion of the package and is mounted on the under surface of the wing and fuselage symmetrically about the centerline of the airplane.

The flight control system is irreversible. The elevons, in conjunction with the canard, provide longitudinal control; differentially deflected elevons provide lateral control; and the twin vertical rudders provide directional control. The right and left elevons are each divided into six segments to prevent control-surface binding under aerodynamic loading. During takeoff and landing, longitudinal control is derived from the elevons alone, and the canard is fixed at 0° incidence with the canard flaps deflected, trailing edge down, at 20°. When the canard flaps are retracted, the canard is geared to the elevons for longitudinal trim and control. The coordinated movement of these surfaces is provided through the control column. Full elevator and canard travel is 15° to -25° and 0° to 6°, respectively. The rudder-control travel varies from ±3°, when the landing gear is retracted, to ±12°, when the gear is extended.

The airplane is equipped with a flight augmentation control system to augment the stability of the vehicle in the pitch, roll, and yaw axes. In the pitch mode, the system actuates only the elevator mode of the elevons; it does not affect the canard.

In normal operation, the XB-70-1 wing tips were undeflected up to high subsonic speeds; deflected to 25° in the high subsonic, transonic, and supersonic region up to a Mach number of approximately 1.4; and deflected to 65° at Mach numbers above 1.4. When the wing tips are deflected, the two outboard segments of the elevons on each tip are faired at zero setting and become part of the folded tip.

The XB-70-1 airplane was manufactured with the wings mounted at a geometric dihedral angle of zero. However, before the initial flight testing, simulator studies indicated that at high Mach number with the stability augmentation off and the wing tips deflected to 65° the airplane was sensitive to the roll and yaw mode with aileron deflection and that approximately 5° of positive geometric dihedral would be required to alleviate the condition. Consequently, a lateral bobweight was installed in the control system to improve the lateral handling qualities. In an attempt to minimize this control problem on the XB-70-2 airplane, a wedge was fitted to the root section of the wing before the wing was installed. The wedge provided the essential 5° of positive dihedral and eliminated the necessity of the lateral bobweight. With this modification to the fixed-wing geometry, the resultant in-flight wing-tip deflections are 30° and 70°.

Propulsion is provided by six YJ93-GE-3 engines, each with a 30,000-pound sea-level static-thrust classification. Each engine has an 11-stage axial-flow compressor, an annular combustion section, a two-stage turbine, and a variable-area converging-diverging exhaust nozzle. An rpm lockup switch, when positioned in the automatic mode, locks all of the engines at 100 percent rpm, regardless of throttle settings, to maintain stable airflow and to improve inlet-shock control above a Mach number of 1.5. The switch is automatically disengaged below a Mach number of 1.3, and the rpm of each engine reverts to throttle control. Below military thrust, throttle movement with the lockup switch engaged varies the exhaust-nozzle area and, in turn, varies engine thrust.

The six engines are mounted side-by-side in the rear of the fuselage in a single nacelle under the center section of the wing. The nacelle is divided into twin, two-dimensional, mixed-compression inlets incorporating variable ramp positions and

throat areas for optimum operation throughout the Mach number range. The left- and right-hand air intake ducts are each equipped with six inlet-air bypass doors on top of each duct just forward and inboard of the leading edge of the vertical tails. These doors are used in conjunction with the controlled width of the two-dimensional throats to control the position of the normal shock in each of the ducts and to match engine-airflow requirements.

SUMMARY OF THE TEST PROGRAM

Figure 2 shows the Mach number — altitude envelope that has been covered by the XB-70 airplanes. For reference, lines of constant indicated airspeed of 300 knots and 600 knots are included. As shown by the dotted area, the flight envelope for the XB-70-1 has been expanded to a Mach number of about 2.85 and an altitude of 68,000 feet. At approximately this speed, the airplane structure has been exposed to a stagnation temperature above 500° F for a total of 49 minutes. The major testing of this airplane has been directed toward stability and control and structural demonstration related to flight safety and toward engine-inlet and environmental-systems tests essential to attain the maximum performance.

The flight envelope of the XB-70-2, represented by the diagonally lined areas, has been expanded to a Mach number of 2.3 and an altitude of 58,000 feet. Flights with this airplane have been directed toward demonstrating handling qualities and checking out the operation of the automatic air-induction system.

DISCUSSION

Stability and Control

In general, the XB-70 pilots have reported that the overall handling qualities of both airplanes in the takeoff and landing regime are satisfactory without the aid of stability augmentation. Trim changes associated with landing gear, wing-tip deflection, and flap manipulation under normal operating conditions have not been considered to be excessive. There has been, however, some indication of an appreciable trim change associated with operations of the inlet bypass door, particularly at high altitude and Mach number. In the early phases of the flight program, the pilot reported the lateral control forces to be light compared with most large airplanes. As a result, the lateral bungee forces were doubled. This modification improved the pitch-to-roll control harmony; however, recent pilot comments have indicated that further investigation of the problem is necessary.

Longitudinal characteristics. — In addition to the general pilot comments, recorded data have shown that an appreciable variation of elevon trim occurs in the transonic region. Figure 3 presents the longitudinal trim measured on the XB-70-1 airplane in terms of elevon and canard deflection as a function of Mach number for various altitudes. The data have been corrected to a constant gross weight of 370,000 pounds and are representative of a mid-center-of-gravity condition. In the transonic region, the elevon varies from 0° to approximately 10°, trailing edge down, while the canard,

which is geared to the elevons, varies between 2° and 0°. When the size of the elevons is considered (fig. 1 and table II), it becomes apparent that this magnitude of deflection can considerably increase the trim drag in the transonic and low supersonic range.

In an attempt to determine the cause of the large trim changes in the transonic speed range, a preliminary analysis of the longitudinal derivatives was made by using an analog-matching technique. Figure 4 presents the pertinent parameters of longitudinal stability C_{m_α} and C_{m_o} and control effectiveness C_{m_δ} plotted against Mach number. For convenience in the analog-matching process, the parameter C_{m_δ} is programed as an equivalent effectiveness parameter in which the elevon and canard effectiveness have been combined into one term. Also shown in this figure are the predicted flexible values for C_{m_α} and C_{m_δ} for comparable test conditions, and the rigid-model wind-tunnel data for C_{m_o}. From the parameters C_{m_α} and C_{m_o}, it may be seen that in the transonic region the static stability provides a somewhat lower nose-down pitching moment than predicted; whereas, the zero-lift pitching moment shows a sharper nose-up trend than predicted. To offset these combined effects requires more trailing-edge-down elevon (nose-down trim) in this region. Also, the flight-derived equivalent effectiveness parameter C_{m_δ} indicates a lower level of effectiveness than was predicted in this Mach range and, in itself, can increase the amount of control required for trim.

Lateral-directional characteristics. – The pilots have commented that at supersonic speed the lateral-directional handling qualities are degraded by an adverse yaw experienced as a result of aileron deflection. Figure 5 presents a comparison, from a preliminary analysis, of the measured stability and control derivatives of the XB-70-1 airplane with predictions as a function of Mach number. For the conditions analyzed, the directional stability C_{n_β} agrees well with the predictions. However, the dihedral effect C_{l_β} is considerably more positive than predicted, and the lateral-control effectiveness $C_{l_{\delta_a}}$ is approximately 30 percent less effective than predicted. Also, the yawing moment produced by the ailerons $C_{n_{\delta_a}}$ is approximately twice the magnitude and of the opposite sign from that predicted. It is believed that this latter effect of adverse yaw, resulting from aileron deflection, in combination with the positive C_{l_β} is producing the objectionable characteristics related to lateral-control sensitivity.

From figure 3, it may be surmised that the large trailing-edge-down elevon deflection for trim, in the transonic and low supersonic speed range, may be responsible for the degree of adverse aileron yaw shown. With the apparent reduction in trailing-edge-down elevon trim as Mach number increases, there should be an improvement in the adverse yawing conditions, resulting from aileron deflection, if a reasonable level of directional stability C_{n_β} is maintained.

The wind-tunnel data in figures 4 and 5 were obtained from faired data generated during a variety of configuration tests. Estimated flexibility corrections for the full-scale airplane have been applied to the wind-tunnel data in conjunction with appropriate corrections to account for minor deviations between the tested models and the final airplane configuration. The cause of the apparent deviation between the predicted and flight-obtained derivative data is not known. However, future flight testing will be

directed toward acquiring more data to establish positive trends and evaluate the influence of the aeroelastic effects.

Takeoff and Landing Performance

On XB-70 flights to date, there has been no attempt to optimize performance during takeoff and landing. In general, during takeoff, the handling qualities have been satisfactory and there appears to be adequate thrust available with all engines operating in the maximum afterburner. In landing, the final approach has normally been along a glide path of between 1.75° and 2.5°. The main runway at Edwards Air Force Base, Calif., has been used unless emergency conditions have dictated the use of the dry lakebed.

Takeoff. – Figure 6 summarizes the takeoff performance corrected to sea-level standard-day conditions. The takeoff distance and lift-off velocity are presented as a function of thrust-to-weight ratio and wing loading, respectively. As shown, the thrust-to-weight ratio varied from approximately 0.29 to 0.38. At the lowest value, 0.29, the takeoff distance was on the order of 8000 feet from brake release. The bottom portion of the figure shows that for these conditions the wing-loading was approximately 80 lb/sq ft and the corresponding lift-off velocity about 210 knots indicated airspeed. In general, the rotation velocity has been between 10 knots and 20 knots below the lift-off speed, and the climb speed, prior to gear and flap retraction, has been 30 knots and 40 knots above the lift-off speed.

Landing. – Figure 7 summarizes landing performance in terms of touchdown velocity as a function of wing loading and the rate of sink at touchdown as a function of the touchdown velocity. Generally, the landings have been made at wing loadings of about 50 lb/sq ft. The velocity at touchdown has been on the order of 180 knots. At the higher wing loading, the previously mentioned lower glide path of approximately 1.75° was used. The plot of touchdown rate of sink shows that the higher touchdown velocity produced a rate of sink between 1.51 ft/sec and 2.5 ft/sec.

During the early portions of the flight program and on initial flights performed after an appreciable layup for maintenance, the pilot of the escort airplane assisted the XB-70 pilot by calling out the estimated XB-70 height above the ground in the final phase of the landing. However, even without this information on recent flights and with the turbulence that has been experienced over the runway, the scatter in the data between the touchdown rates of 1 ft/sec to 4 ft/sec is not considered to be excessive. These rates are well within the repeated level of touchdown rates of sink experienced by the current jet fleets. It should be pointed out, however, that during these landings, the pilots did not attempt to land within the first 1000 feet of the runway threshold.

Ground effect. – From the landing data that have been accumulated and from specified conditions on future flights, the ground effect in the final phase of landing will be assessed. If the airplane is flown at a constant angle of attack as it approaches the runway, the ground effect, if present, produces a change in the downwash characteristics which results in an incremental increase in lift that can be beneficial in arresting the sink rate or detrimental in producing a severe nose-down pitching moment. Movies of the landings and onboard data have indicated that a reasonable level of ground effect can be demonstrated by the XB-70. In figure 8, which presents main-landing-gear

height above the runway as a function of rate of sink, the rate of sink at 100 feet is approximately 11.5 ft/sec. This rate is reduced to 1.5 ft/sec at touchdown, with no appreciable change in angle of attack. The angle of attack for this portion of the landing approach to touchdown was about 9.5°, while the pitch angle varied between 7.5° and 9°. Also, in this region of the flight path the thrust was essentially constant.

Figure 9 presents the measured change in lift, derived from onboard and Askania phototheodolite data, as a function of altitude for the landing shown in figure 8. At touchdown, the lift appears to have increased by at least 15 percent, which compares favorably with predictions. Also, as an initial check of these data, the change in lift was calculated from data obtained during a low pass over the runway. These data, represented by the diamond symbol at an altitude of 30 feet, show good agreement with data derived from the continuous landing.

On the basis of the data shown in figures 8 and 9, there appears to be an appreciable influence of ground effect through the large reduction in sink rate and an apparent increase in lift. However, with the meager data obtained to date, it is difficult to draw a firm conclusion. At this stage of the investigation, the control inputs and forces exerted by the pilot during the flare tend to mask the true level of ground effect experienced. The pilot has commented that he is not completely aware of the influence of ground effect and believes that he is, in fact, providing a major contribution to the final flare and to arresting the final sink rate. However, in view of the relatively small change in airplane attitude that has been observed, it is believed that a portion of the pilot's effort is that required to oppose the increased nose-down pitching moment produced by the influence of the ground plane. Also, the resultant deflection of the elevons with no increase in angle of attack should normally reduce the overall lift. In this case, however, the lift appears to increase.

Propulsion System

The XB-70 propulsion system incorporates a mixed-compression inlet. Figure 10 is a schematic drawing of one-half of the symmetrical two-dimensional inlet which supplies airflow to three of the six engines. For the design cruise conditions, compression takes place through a series of shock waves generated in the forward portion and inside the inlet. The final or terminal shock is positioned near the throat, which can be controlled to the appropriate height for the flight Mach number. Just forward of the engine-compressor faces are variable bypass doors, which are used to match the captured inlet air with the airflow required by the engines. The excess captured inlet air is bypassed overboard. Another important function of the bypass doors is to aid in positioning the terminal shock for optimum total-pressure recovery. The best terminal-shock location for optimum recovery approaches the operating boundary limit where the least disturbance can produce an instability. With an unstable condition, the terminal shock may be moved forward to the extent that the initial oblique shock will be forced outside of the inlet lip, thereby "unstarting" the inlet. Such an "unstart" not only affects the efficiency of the propulsion system but may have a pronounced effect on the handling qualities of the airplane. For safety of flight, a compromise must be made between maximum inlet performance and inlet stability.

In the XB-70 flight program to date, optimum pressure recovery has been sacrificed for a more stable inlet operation to insure safety during maneuvering flight or

when specific stability and control tests were performed. Figure 11 presents, as a function of Mach number, some of the preliminary pressure-recovery data acquired. The data represented by the open symbols were obtained with the inlet throat and related bypass area adjusted so that the normal shock would be in the "low" performance range. With this inlet setting, as shown in the previous figure, the normal shock is located in the aft portion of the throat. In this location, the normal shock appears to be more stable during maneuvering flight, and the recovery is between 5 percent and 10 percent below that for the "normal" performance range.

As indicated by the solid symbols, the XB-70 inlet has been operated in the region of the "normal" performance line and above, which is essentially midway between the "high" and "low" performance ranges. For these test conditions the pressure recovery varied from approximately 87 percent at $M = 2.3$ to 78 percent at $M = 2.8$, which is somewhat below that predicted for optimum performance. However, these data were obtained while the airplane was held in steady (equilibrium) flight conditions or during transient conditions just prior to a demonstration of an inlet "unstart."

Thermal Environment

The most severe temperatures to which the XB-70 has been exposed were encountered on a flight in which the XB-70-1 remained in steady level flight at a Mach number of 2.8 for 20 minutes. Figure 12 shows a planform of the under surface of the airplane and the locations at which the temperature measurements to be discussed were made. These measurements are representative of the 143 thermocouples on the XB-70-1 airplane and were made at a location on the forward portion of the fuselage, two locations on the same wing chord, and on the wing-fold actuator.

Figure 13 is a time history of the Mach number and altitude profile flown and the variation of the measured temperatures including the total stagnation temperature, which reached a maximum of 514° F. The two temperature measurements at the common wing chord, which are approximately 14 inches apart, show that the leading edge responds rapidly to the total temperature variation; at the maximum temperature levels, there is a gradient between the two chord stations of approximately 100° F. The slower response of the aft measurement and the indicated temperature gradient is caused by the heat-sink characteristics of the fuel in a wing tank in this area. The wing-fold actuator represents a typical massive element with very slow thermal response. The actuator does not reach its peak temperature until 24 minutes after maximum total temperature has been attained, and is still at 150° F at landing.

Figure 14 summarizes the variation of the wing and forward-fuselage surface temperatures with total temperature and compares the predictions for flight between Mach numbers of 2 and 3. At a total temperature of 510° F, the measured wing leading edge and fuselage temperatures agree with predictions for these equilibrium conditions. It appears that this correlation will be maintained, on the basis of the extrapolation, to a Mach number of 3. Assuming that the temperatures at the aft-wing station would show the same agreement, the indicated wing surface will reach approximately 340° F at $M = 3$, and the temperature gradient between the two wing stations will increase to almost 200° F. This latter assumption, however, will depend on the fuel heat-sink qualities, which are yet to be determined.

The highest fuel temperature measured in the tanks during this flight was approximately 130° F. The maximum hydraulic fluid temperature was 360° F.

Internal Noise

Throughout the flight program, the XB-70 crew commented on the variation of the noise level inside the airplane, particularly in the transonic speed range. A portion of the noise is attributed to the turbulent boundary layer generated by the windshield. This noise, of course, can be alleviated by raising the windshield ramp to fair the nose section for supersonic flight.

As part of the NASA XB-70 study, microphones have been installed in two locations in the forward portion of the fuselage—the cockpit and ballast bay (fig. 15). In the ballast bay, the microphone is located between two rib stations and faces the uninsulated skin surface. In the cockpit, the microphone is installed between the pilot and copilot approximately 2 feet from the nearest fuselage wall. As shown in figure 15, the cockpit area is insulated for heat and noise attenuation from the exterior to the interior by a 2-inch layer of fiber glass, a 1-inch air gap, 1/2 inch of fiber glass, a 3/4-inch air gap, and, finally, by the transpiration wall.

Figure 16 shows the overall sound pressure levels measured at the two microphone locations over the Mach number range covered during typical climb profiles to an altitude of approximately 65,000 feet. It may be observed that in the transonic speed range between Mach numbers of 0.8 and 1.2 the noise level is reduced by approximately 10 decibels. As would be expected, the insulated wall in the cockpit reduced the sound pressure by as much as 15 decibels below that measured in the ballast bay. However, the overall reduction in sound pressure level from subsonic to supersonic flight appears to be somewhat greater in the ballast bay.

For comparison, the average sound pressure level measured in the cockpit of a current subsonic jet at $M \approx 0.85$ and an altitude of 20,000 feet is illustrated by the diagonally lined area. In the subsonic region, the XB-70 exhibits noise levels approximately 12.5 decibels higher than the current jet transport; in the supersonic region, the XB-70 sound pressure levels are reduced to approximately the same level as those of the transport.

Figure 17 presents a preliminary octave-band analysis in terms of sound pressure versus frequency for the two XB-70 microphone stations at $M = 0.9$ and $M = 2.5$. With the exception of the ballast-bay data at $M = 0.9$ and a frequency of 500 cps, the sound pressure levels appear to be relatively constant over the frequency range. Also, as indicated in the previous figure, the subsonic to supersonic reduction in sound pressure level is considerably greater in the ballast bay than that measured in the cockpit area.

Runway Noise

To investigate the noise problems in and around an airport, a series of noise measurements is being made at Edwards Air Force Base with various types of airplanes, including the XB-70. NASA, with the assistance of the U.S. Air Force Flight

Test Center, installed an acoustical measuring system under the normal landing flight path and along the main runway. The instrumentation layout is shown in figure 18. Twelve microphone stations are positioned symmetrically in pairs at 5000-foot intervals along and beyond the runway. The lateral distance between the pairs of microphones varies from 310 feet to 1000 feet. The noise measured by each microphone is amplified and transmitted via an underground cable system to a tape recorder in a van.

An example of the data obtained from this system is shown in figure 19, in which XB-70 takeoff and landing noise is plotted in terms of sound pressure level at the center frequencies of the respective octave bands. Noise measured by microphones 1 and 2 is presented for two takeoffs in which the flight profile and weather conditions were similar. Repeatability of the data is good. The data show that at an average slant range from the microphone of 750 feet, the average overall sound pressure level (solid symbols in the upper left) is 138 decibels.

The noise measured by microphones 9 and 10 for two landings is shown in the bottom portion of the figure. Inasmuch as complete space-positioning data were not available for the airplane when passing these microphones, the spread in the measured sound pressure levels is difficult to explain. In view of the 860-foot separation of the stations and the fact that one landing was made in a 12-knot crosswind, it is reasonable to assume that a portion of the 6-decibel discrepancy in the data is due to the "crab" angle and runway offset experienced. At an estimated slant range of 540 feet from microphone stations 9 and 10, the average overall sound pressure level (solid symbols at the left) is 108.5 decibels.

Sonic Boom

In conjunction with the XB-70 flight tests, measurements of the sonic-boom pressure signatures are being obtained in regions of the flight envelope comparable to those predicted for supersonic-transport designs. The principal objective of the program is to obtain data with which to improve present methods of predicting sonic-boom overpressures.

Figures 20(a) to 20(c) present typical measured XB-70 overpressure signatures. The Mach number varies from 1.22 to 1.86, and height above the ground varies from 27,000 feet to 48,000 feet. Figure 20(a) shows three shocks in the positive portion of the signature, figure 20(b) shows two shocks, and figure 20(c) shows only one shock. Data in figures 20(a) and 20(b) were obtained in the near field of the XB-70 pressure signature; data in figure 20(c) were from the far field. The initial significance of these data is that the near-field effect measured on the ground was obtained with the XB-70 at a somewhat greater altitude than anticipated.

To illustrate a potential influence of the near-field effect on the reduction of bow-wave overpressures, figures 21(a) and 21(b) compare the XB-70 near-field pressure signature with the B-58 far-field pressure signature. The maximum overpressure of the XB-70 is only slightly greater than the B-58 bow-wave overpressure, whereas the XB-70 weight is approximately 3.5 times that of the B-58. Both airplanes were at the same altitude and Mach number, with the B-58 only about 800 feet behind the XB-70.

XB-70 sonic-boom data have been obtained over a Mach number range from approximately 1.2 to 2.6 and altitudes above the ground from 27,000 feet to 64,000 feet.

The amount of data obtained to date is limited; much additional data will be required to assess the effects of Mach number, altitude, gross weight, and weather.

CONCLUDING REMARKS

In the initial flight testing of the XB-70 airplanes, preliminary data were obtained on stability and control characteristics, general performance, inlet operations, and conditions associated with the operational environment.

In general, the XB-70 handling characteristics and performance were considered to be satisfactory throughout the portions of the flight envelope tested; however, excessive longitudinal elevon trim and associated adverse aileron yaw characteristics were noted, particularly in the transonic speed range.

Although no attempt was made to optimize takeoff and landing performance, there appeared to be adequate control and thrust available in these flight regimes. Approach and landing speeds were 40 knots to 50 knots higher than those of current jet transports, and sink rates at touchdown were well within the range of 1 ft/sec to 4 ft/sec experienced by the jets. A preliminary analysis indicated that the XB-70 experiences an incremental increase in lift near the ground plane; however, additional studies and flight testing will be required before the specific increase can be assessed.

Inlet operations in the early phase of the testing were limited to a safe region of shock position. A sacrifice of 5 to 10 percent in pressure recovery was accepted below a normal inlet operational range, particularly during maneuvering flight. Some data were acquired at near-optimum pressure-recovery conditions; however, these data were obtained close to the inlet stability boundary just prior to inlet "unstart" conditions with the airplane held in stabilized flight.

The temperatures measured at several locations throughout the structure of the XB-70 compared favorably with predictions. Also, temperature data indicated an appreciable delay in the response of the more dense structure, such as the wing-fold actuator, to the variation in thermal gradients.

In the transition from subsonic to supersonic speed, the internal noise levels were reduced by approximately 10 decibels between Mach numbers of 0.80 and 1.2; in the supersonic range, the level of the cockpit noise was the same as that measured in current jet transports during cruise flight.

Preliminary noise levels measured for an average slant range from the microphones of 750 feet during takeoff and 540 feet during landing were 138 and 110 decibels, respectively. Additional flight testing is required to better define the effects of such factors as wind, weather, airplane position, and power setting.

Sonic-boom data indicated that near-field effects measured on the ground may be experienced at higher aircraft operational altitudes than anticipated.

Flight Research Center,
National Aeronautics and Space Administration,
Edwards, Calif., March 21, 1966.

REFERENCES

1. Sisk, Thomas R.; Irwin, Kirk S.; and McKay, James M.: Review of the XB-70 Flight Program. Conference on Aircraft Operating Problems, NASA SP-83, 1965, pp. 183-192.

2. Tanner, Carole S.; and McLeod, Norman J.: Preliminary Measurements of Take-Off and Landing Noise From a New Instrumented Range. Conference on Aircraft Operating Problems, NASA SP-83, 1965, pp. 83-90.

TABLE I. – NASA XB-70 FLIGHT RESEARCH PROGRAM

Flight dynamics	Performance and propulsion	Loads	Environmental factors
Aerodynamic derivatives	Takeoff and landing	Landing loads and dynamics	Runway noise
Handling-qualities criteria	Lift and drag characteristics	Dynamic loads	Sonic boom
Flight control systems	Skin friction	Panel response	Thermal environment
Guidance and display	Base pressure survey	Flight loads and structural evaluation	Internal cabin environment
	Boundary-layer transition		Boundary-layer noise
	Air-induction system		
	Thrust determination		
	Engine-to-engine interactions		

TABLE II. – GEOMETRIC CHARACTERISTICS OF THE XB-70 AIRPLANES

Total wing –		
Total area (includes 2482. 34 sq ft covered by fuselage but not 33. 53 sq ft of wing ramp area), sq ft		6297. 15
Span, ft		105
Aspect ratio		1. 751
Taper ratio		0. 019
	XB-70-1	XB-70-2
Dihedral angle, deg	0	5
Root chord (wing station 0), ft		117. 76
Tip chord (wing station 630), ft		2. 19
Mean aerodynamic chord (wing station 213. 85), in.		942. 38
Fuselage station of 25-percent wing mean aerodynamic chord, in.		1621. 22
Sweepback angle, deg:		
Leading edge		65. 57
25-percent element		58. 79
Trailing edge		0
Incidence angle, deg:		
Root (fuselage juncture)		0
Tip (fold line and outboard)		-2. 60
Airfoil section:		
Root to wing station 186 (thickness-chord ratio, 2 percent)	0. 30 - 0. 70 HEX (MOD)	
Wing station 460 to 630 (thickness-chord ratio, 2. 5 percent)	0. 30 - 0. 70 HEX (MOD)	
Inboard wing –		
Area (includes 2482. 34 sq ft covered by fuselage but not 33. 53 sq ft wing ramp area), sq ft		5255. 47
Span, ft		63. 44
Aspect ratio		0. 766
Taper ratio		0. 407
	XB-70-1	XB-70-2
Dihedral angle, deg	0	5
Root chord (wing station 0), ft		117. 76
Tip chord (wing station 380. 62), ft		47. 94
Mean aerodynamic chord (wing station 163. 58), in.		1053
Fuselage station of 25-percent wing mean aerodynamic chord, in.		1538. 29
Sweepback angle, deg:		
Leading edge		65. 57
25-percent element		58. 79
Trailing edge		0
Airfoil section:		
Root (thickness-chord ratio, 2 percent)	0. 30 - 0. 70 HEX (MOD)	
Tip (thickness-chord ratio, 2. 4 percent)	0. 30 - 0. 70 HEX (MOD)	

TABLE II. – GEOMETRIC CHARACTERISTICS OF THE XB-70 AIRPLANES – Continued

Mean camber (leading edge), deg:		
Butt plane 0		0.15
Butt plane 107		4.40
Butt plane 153		2.75
Butt plane 257		2.60
Butt plane 367 to tip		0
Outboard wing –		
Area (one side only), sq ft		520.84
Span, ft		41.56
Aspect ratio		1.658
Taper ratio		0.046
Dihedral angle, deg		5
Root chord (wing station 380.62), ft		47.94
Tip chord (wing station 630), ft		2.19
Mean aerodynamic chord (wing station 467.37), in.		384.25
Sweepback angle, deg:		
Leading edge		65.57
25-percent element		58.79
Trailing edge		0
Airfoil section:		
Root (thickness-chord ratio, 2.4 percent)		0.30 - 0.70 HEX (MOD)
Tip (thickness-chord ratio, 2.5 percent)		0.30 - 0.70 HEX (MOD)
Down deflection from wing reference plane, deg		0, 30, 70
Skewline of tip fold, deg:		
Leading edge in		1.5
Leading edge down		3
Wing-tip area in wing reference plane (one side only), sq ft:		
Rotated down 30°		472.04
Rotated down 70°		220.01
	Wing tips	
	Up	Down
Elevons (data for one side):		
Total area aft of hinge line, sq ft	188.45	132.44
Span, ft	20.44	13.98
Inboard chord (equivalent), in.	116	116
Outboard chord (equivalent), in.	116	116
Sweepback angle of hinge line, deg	0	0
Deflection, deg –		
As elevator	-25 to 15	-25 to 15
As aileron with elevators at ±15° or less	-15 to 15	-15 to 15
As aileron with elevators at -25°	-5 to 5	-5 to 5
Total	-30 to 30	-30 to 30
Canard –		
Area (includes 150.31 sq ft covered by fuselage), sq ft		415.59
Span, ft		28.81
Aspect ratio		1.997
Taper ratio		0.388

TABLE II. – GEOMETRIC CHARACTERISTICS OF THE XB-70 AIRPLANES – Continued

Dihedral angle, deg	0
Root chord (canard station 0), ft	20.79
Tip chord (canard station 172.86), ft	8.06
Mean aerodynamic chord (canard station 73.71), in.	184.3
Fuselage station of 25-percent canard mean aerodynamic chord	553.73
Sweepback angle, deg:	
Leading edge	31.70
25-percent element	21.64
Trailing edge	-14.91
Incidence angle (nose up), deg	0 to 6
Airfoil section:	
Root (thickness-chord ratio 2.5 percent)	0.34 - 0.66 HEX (MOD)
Tip (thickness-chord ratio 2.52 percent)	0.34 - 0.66 HEX (MOD)
Ratio of canard area to wing area	0.066
Canard flap (one of two):	
Area (aft of hinge line), sq ft	54.69
Ratio of flap area to canard semi-area	0.263
Vertical tail (one of two) –	
Area (includes 8.96 sq ft blanketed area), sq ft	233.96
Span, ft	15
Aspect ratio	1
Taper ratio	0.30
Root chord (vertical-tail station 0), ft	23.08
Tip chord (vertical-tail station 180), ft	6.92
Mean aerodynamic chord (vertical-tail station 73.85), in.	197.40
Fuselage station of 25-percent vertical-tail mean aerodynamic chord	2188.50
Sweepback angle, deg:	
Leading edge	51.77
25-percent element	45
Trailing edge	10.89
Airfoil section:	
Root (thickness-chord ratio 3.75 percent)	0.30 - 0.70 HEX (MOD)
Tip (thickness-chord ratio 2.5 percent)	0.30 - 0.70 HEX (MOD)
Cant angle, deg	0
Ratio vertical tail to wing area	0.037
Rudder travel, deg:	
With gear extended	±12
With gear retracted	±3
Fuselage (includes canopy) –	
Length, ft	189
Maximum depth (fuselage station 878), in.	106.92
Maximum breadth (fuselage station 855), in.	100
Side area, sq ft	939.72
Planform area, sq ft	1184.78
Duct –	
Length, ft	104.84
Maximum depth (fuselage station 1375), in.	90.75
Maximum breadth (fuselage station 2100), in.	360.70

TABLE II. – GEOMETRIC CHARACTERISTICS OF THE XB-70 AIRPLANES – Concluded

Side area, sq ft	716.66
Planform area, sq ft	2342.33
Inlet captive area (each), sq in.	5600
Surface areas (net wetted), sq ft –	
Fuselage and canopy	2871.24
Duct	4956.66
Wing, wing tips, and wing ramp	7658.44
Vertical tails (two)	936.64
Canard	530.83
Tail pipes	340.45
Total	17,294.26
Landing gear –	
Tread, ft	23.17
Wheelbase, in.	554.50
Tire size:	
Main gear (8)	40 x 17.5-18
Nose gear (2)	40 x 17.5-18

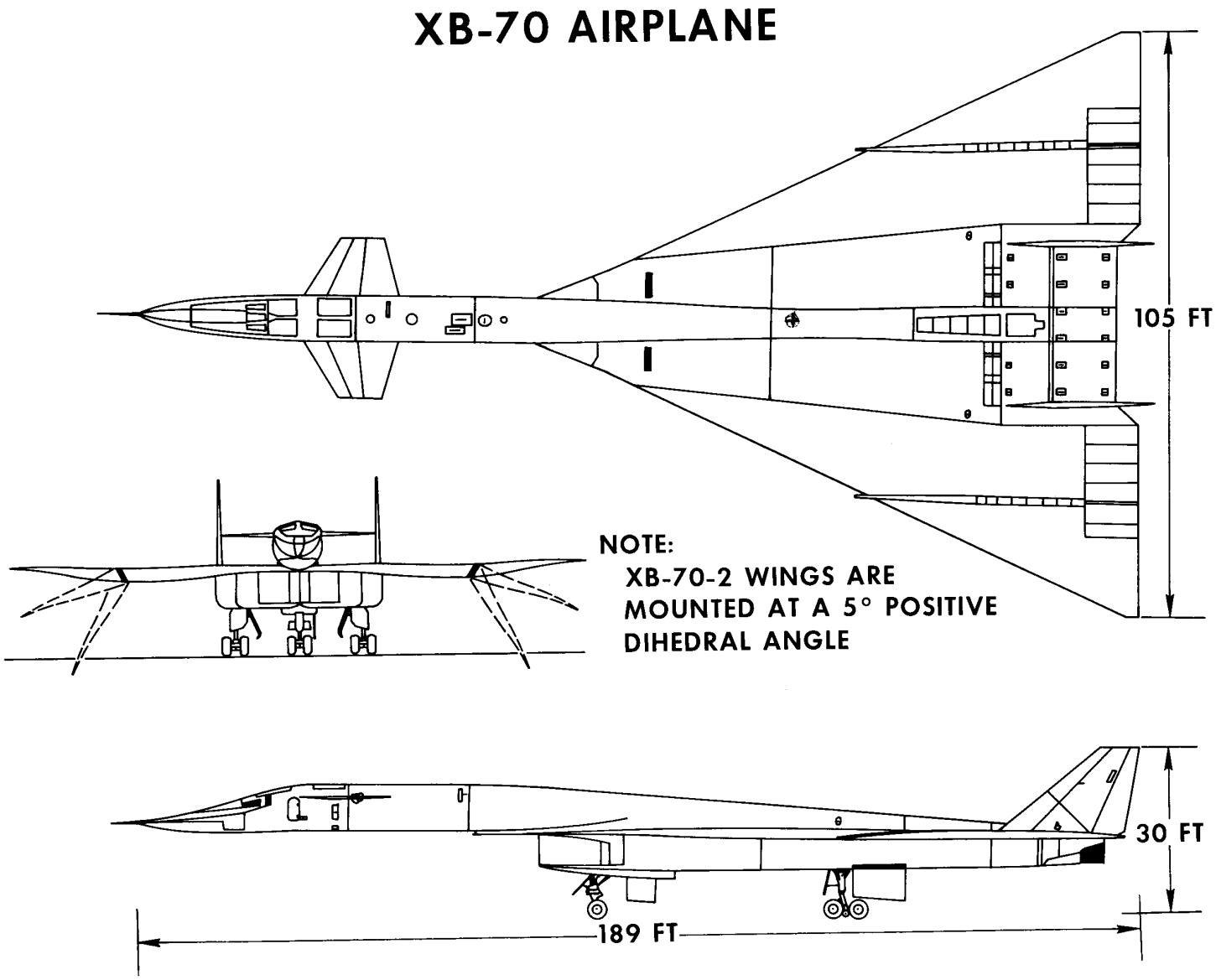

Figure 1. – Three-view drawing of the XB-70-1 airplane.

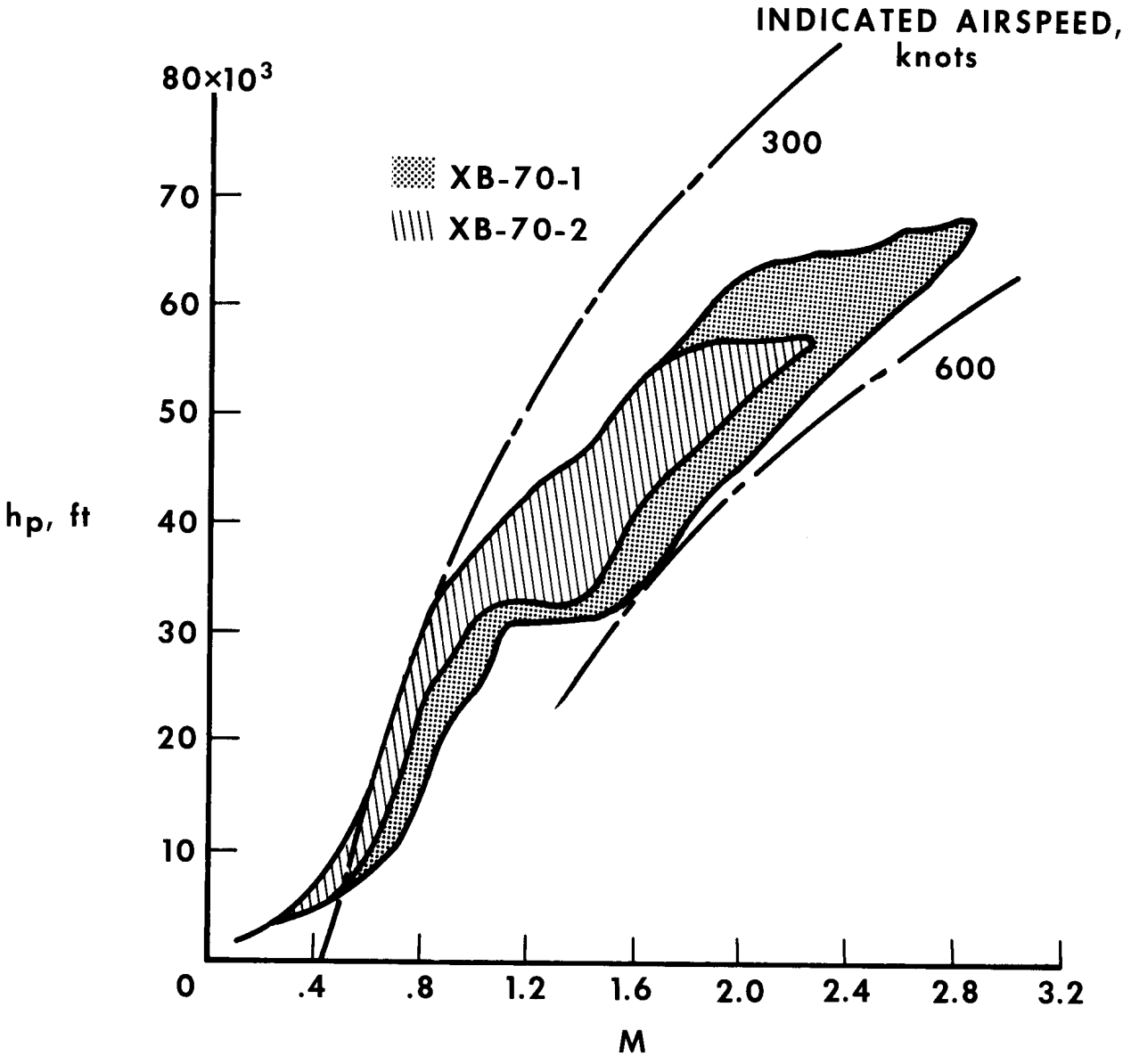

Figure 2.– Test envelope covered during the initial phase of the flight test program.

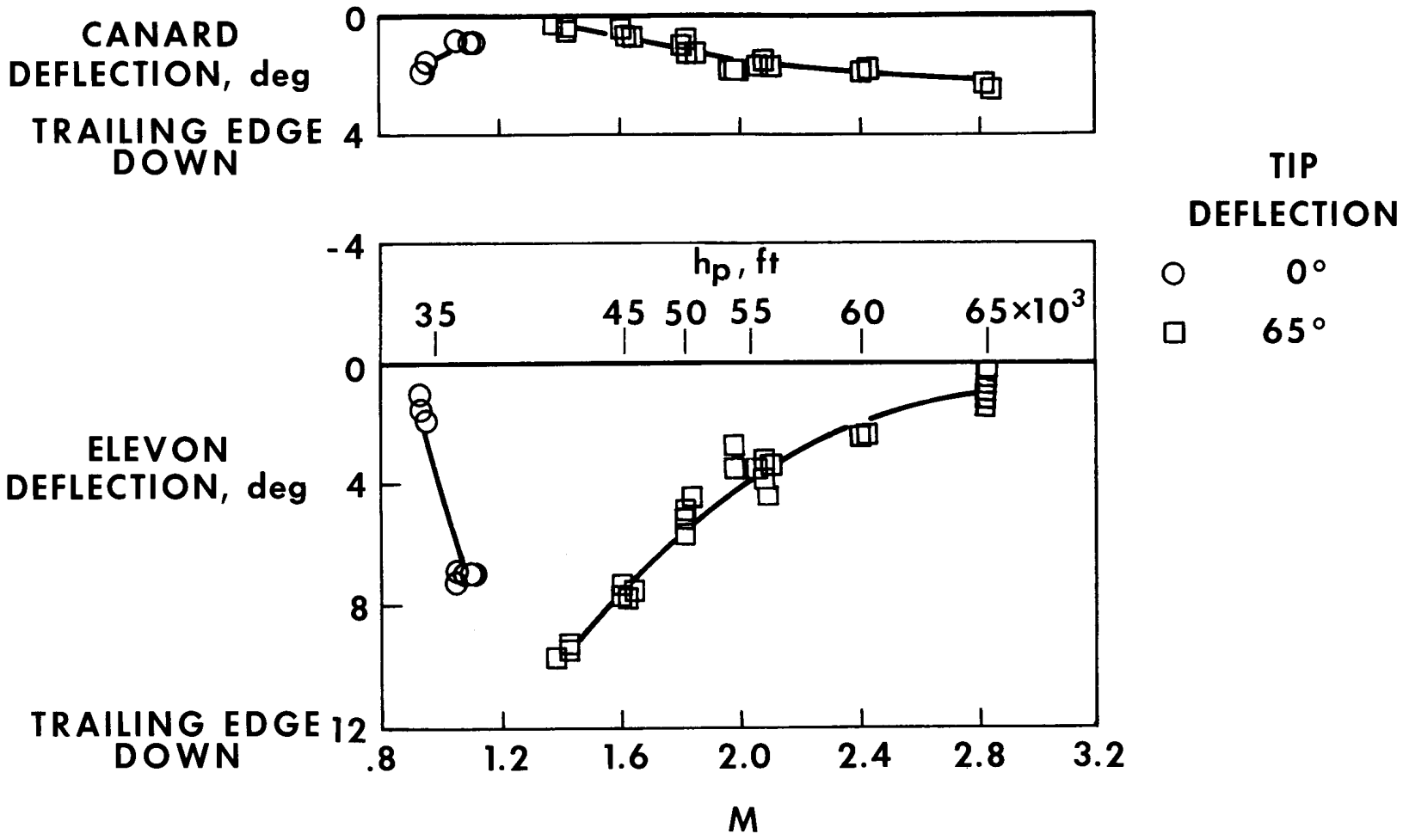

Figure 3. – Summary of the longitudinal-trim characteristics of the XB-70-1 airplane with wing tips deflected at 0° and 65°. Gross weight = 370,000 lb; center of gravity = 22.2-percent mean aerodynamic chord.

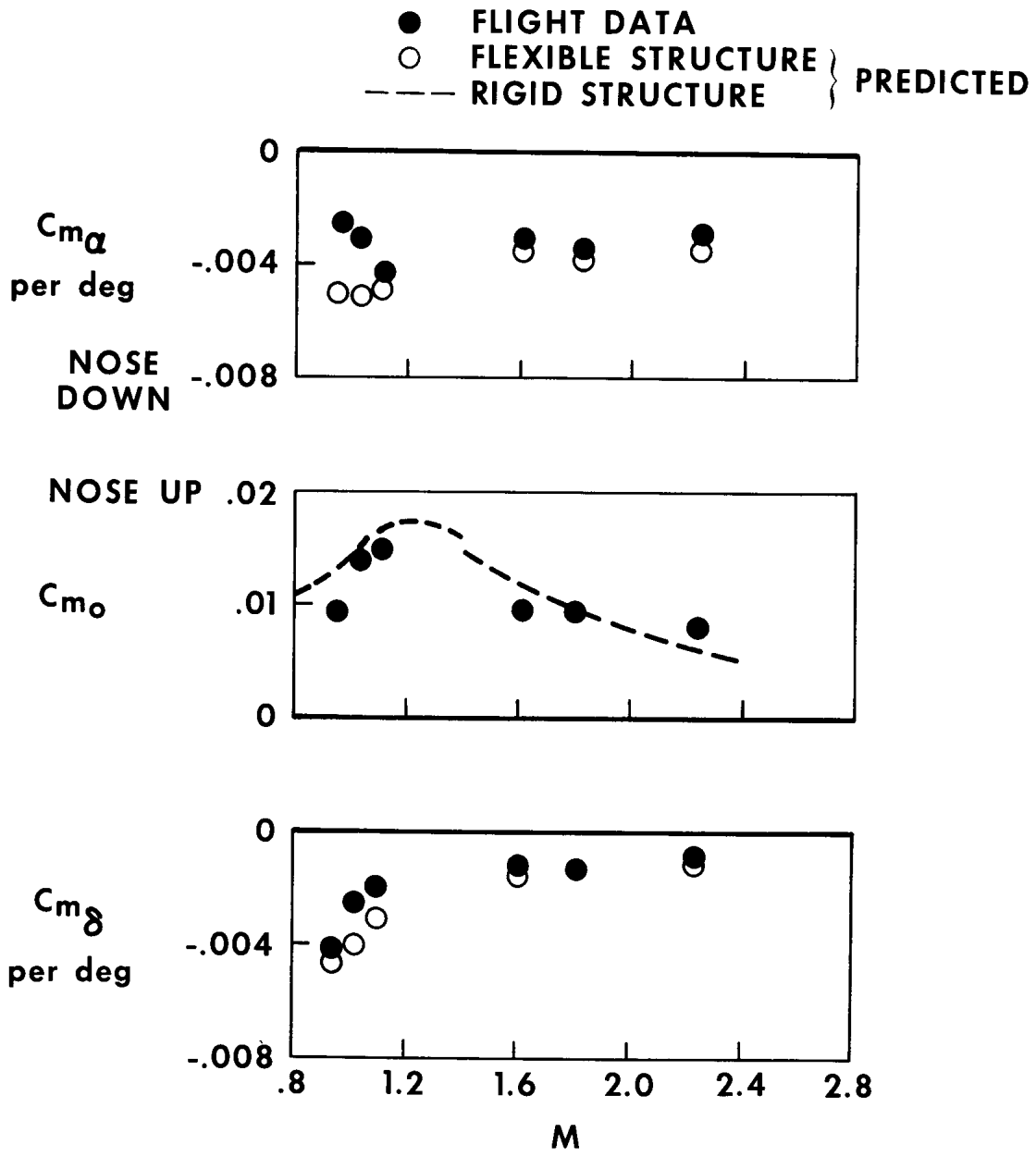

Figure 4. – Comparison of longitudinal stability and control derivatives of the XB-70-1 airplane with predictions derived from wind-tunnel data.

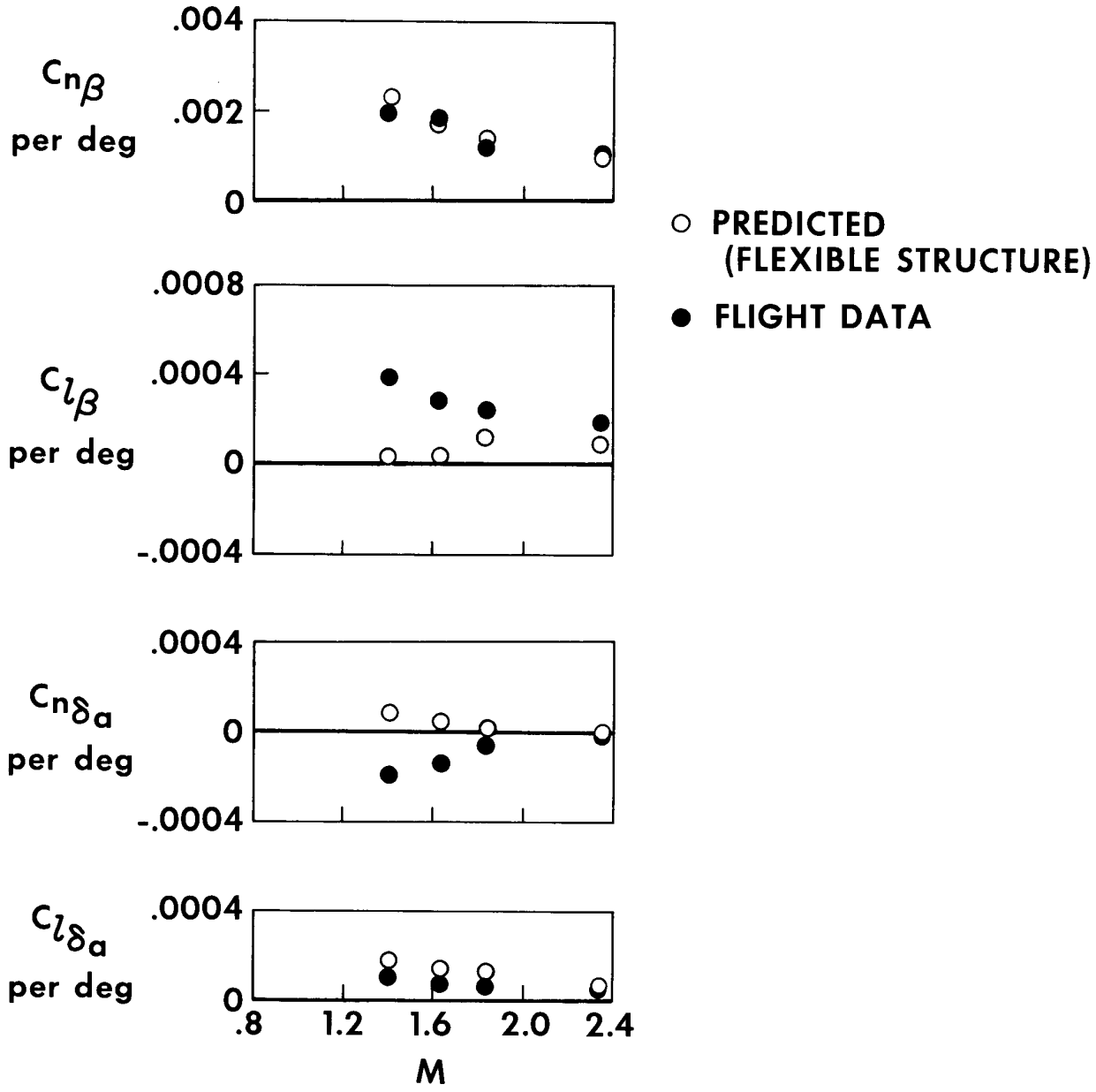

Figure 5. – Comparison of lateral-directional stability and control derivatives of the XB-70-1 airplane with predictions derived from wind-tunnel data.

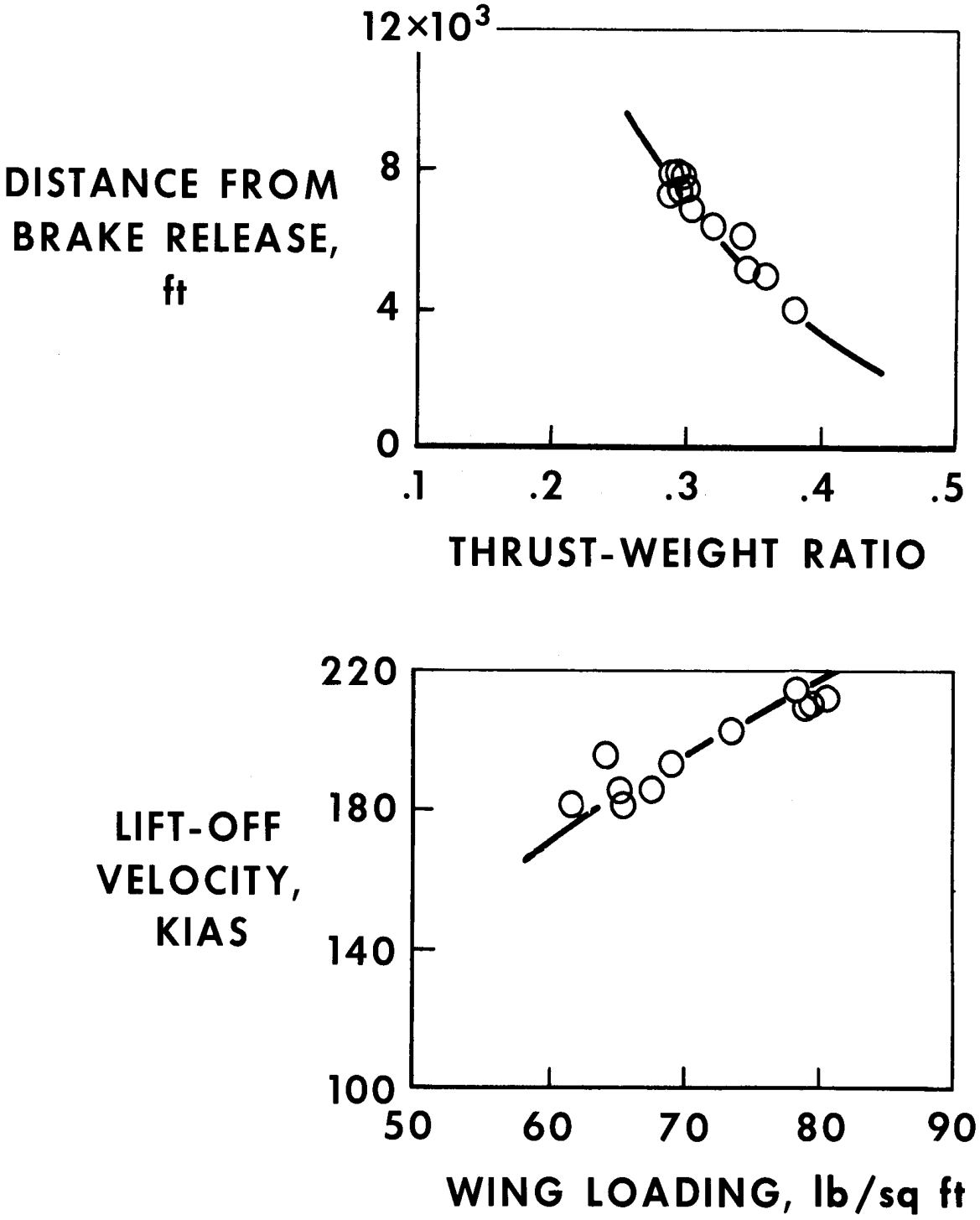

Figure 6. – Summary of takeoff performance characteristics corrected to sea-level standard-day conditions.

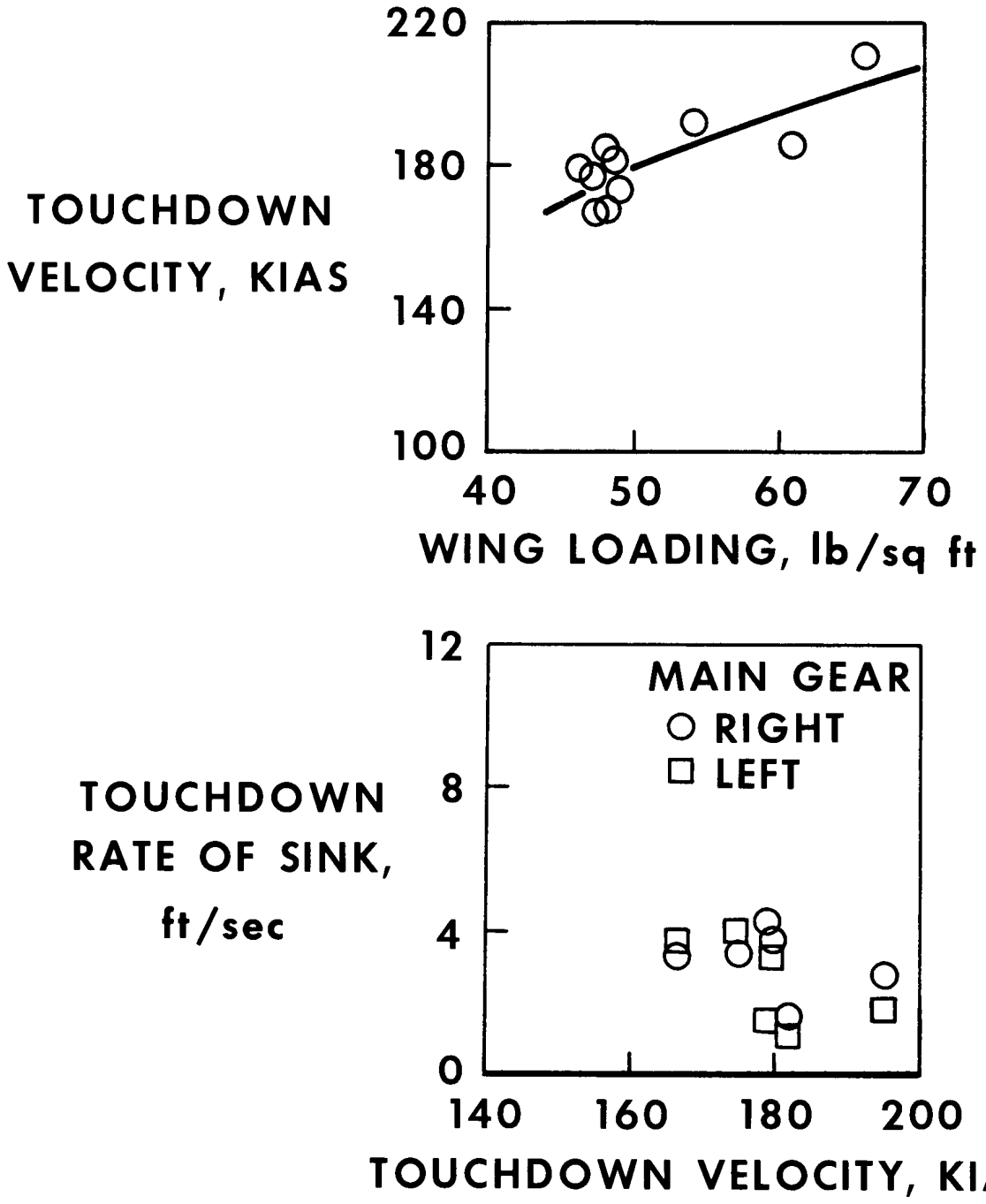

Figure 7. – Summary of landing performance characteristics corrected to sea-level standard-day conditions.

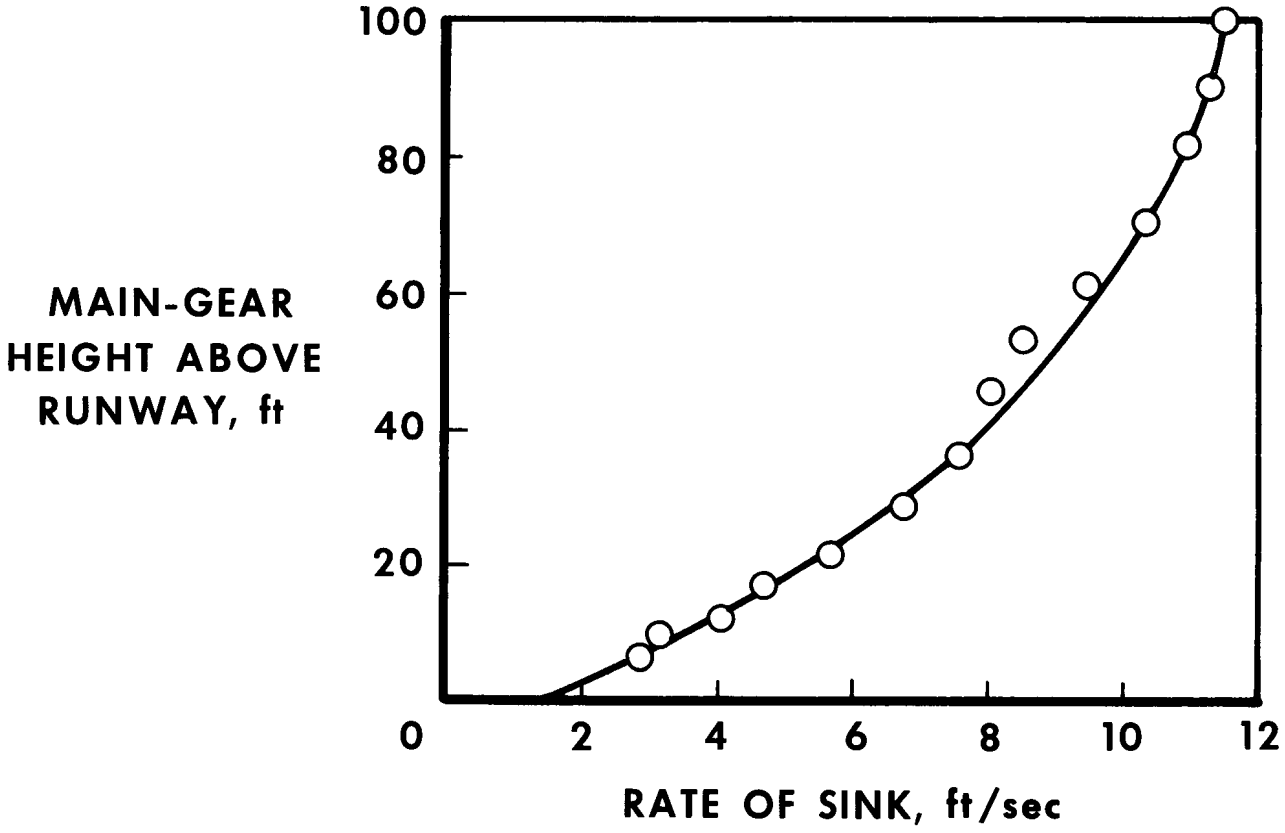

Figure 8. – Typical rate-of-sink characteristics measured during the final phase of landing. $\alpha \approx 9.5°$; pitch angle = 7.5° to 9°.

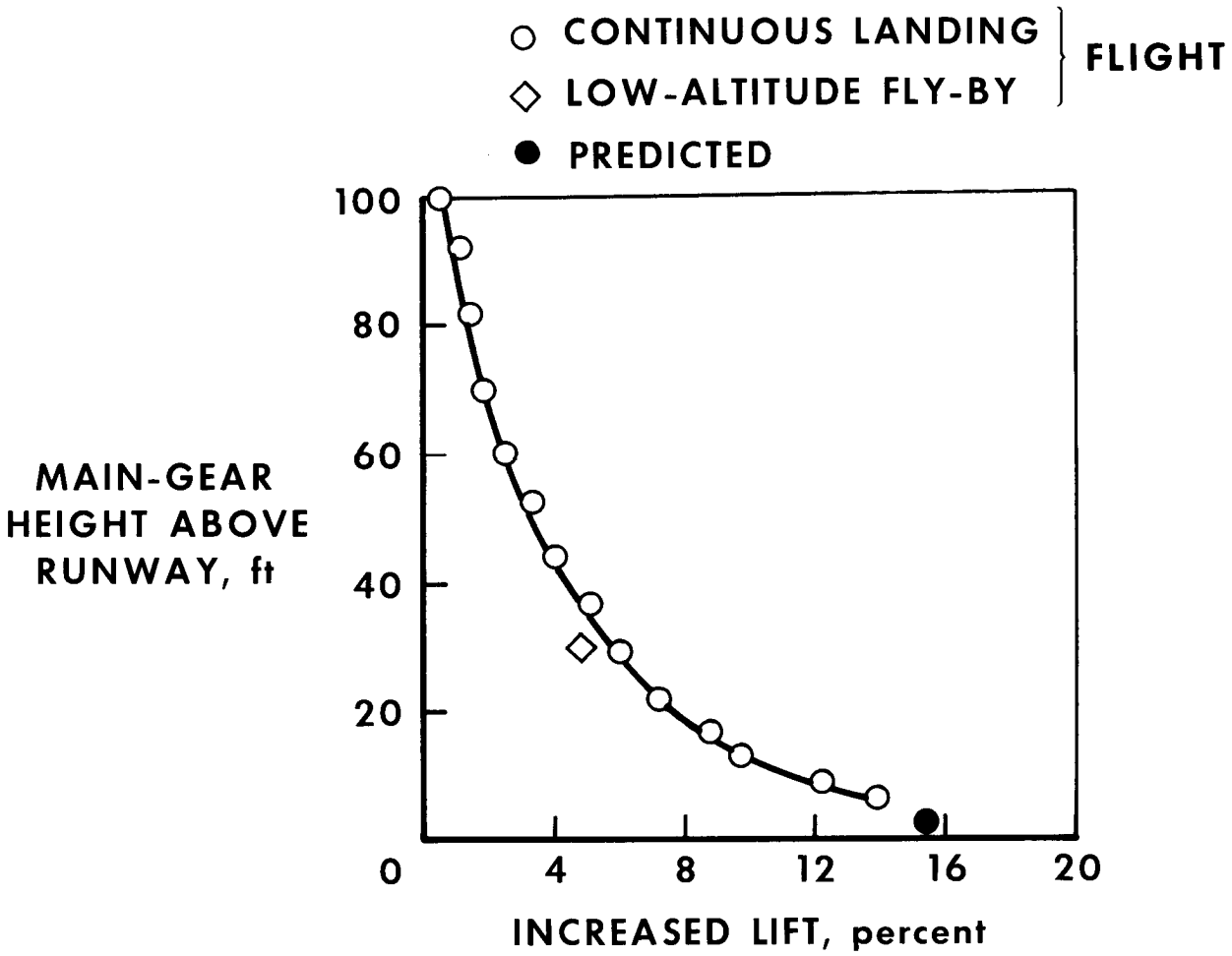

Figure 9.– Incremental lift measured near the ground plane.

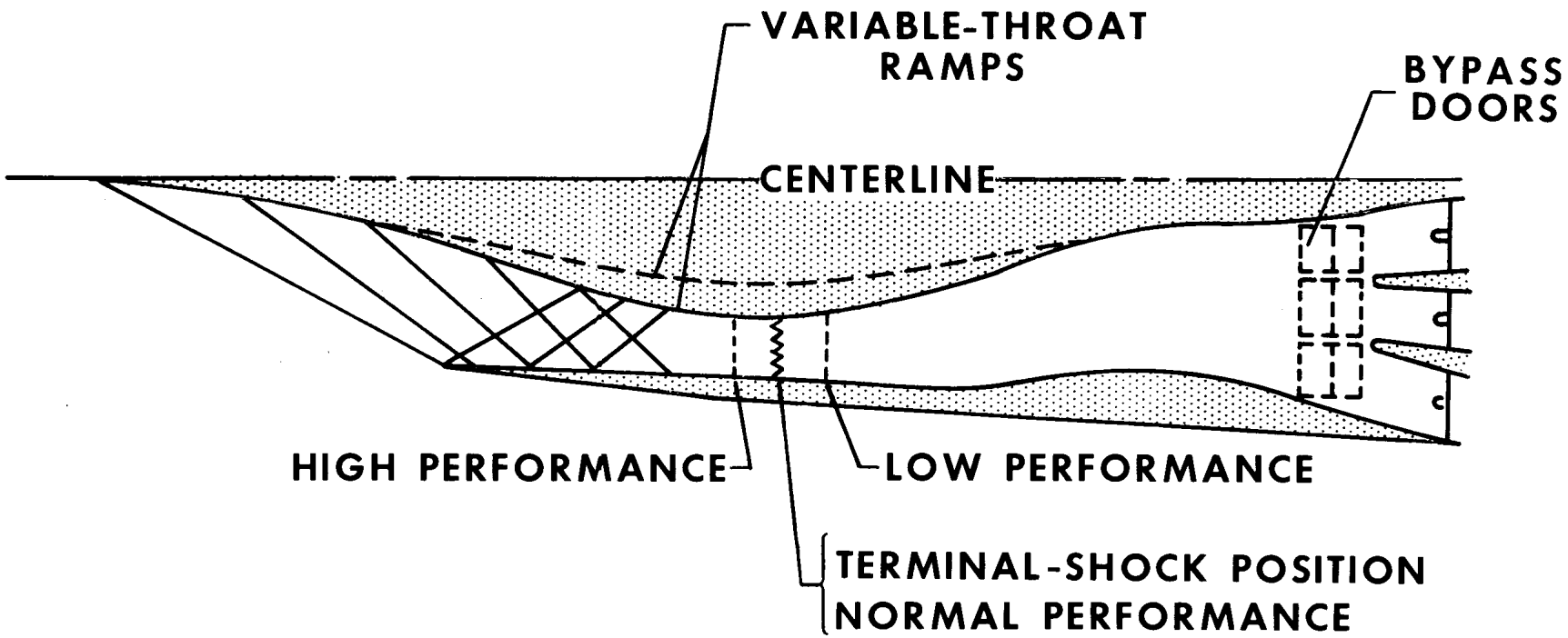

Figure 10. – Schematic of the air-induction inlet and shock-wave system. Top view, left side.

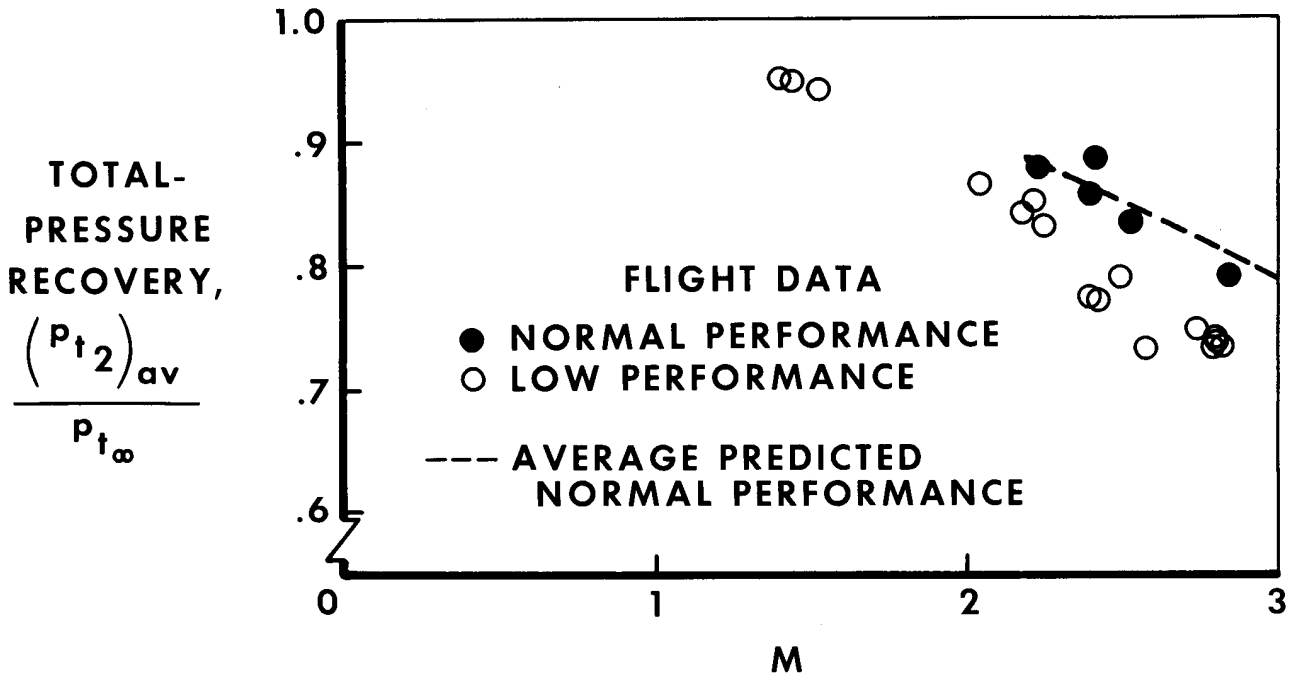

Figure 11. – Summary of total-inlet pressure-recovery data acquired with the normal and low performance settings of the inlet throat ramp and bypass doors.

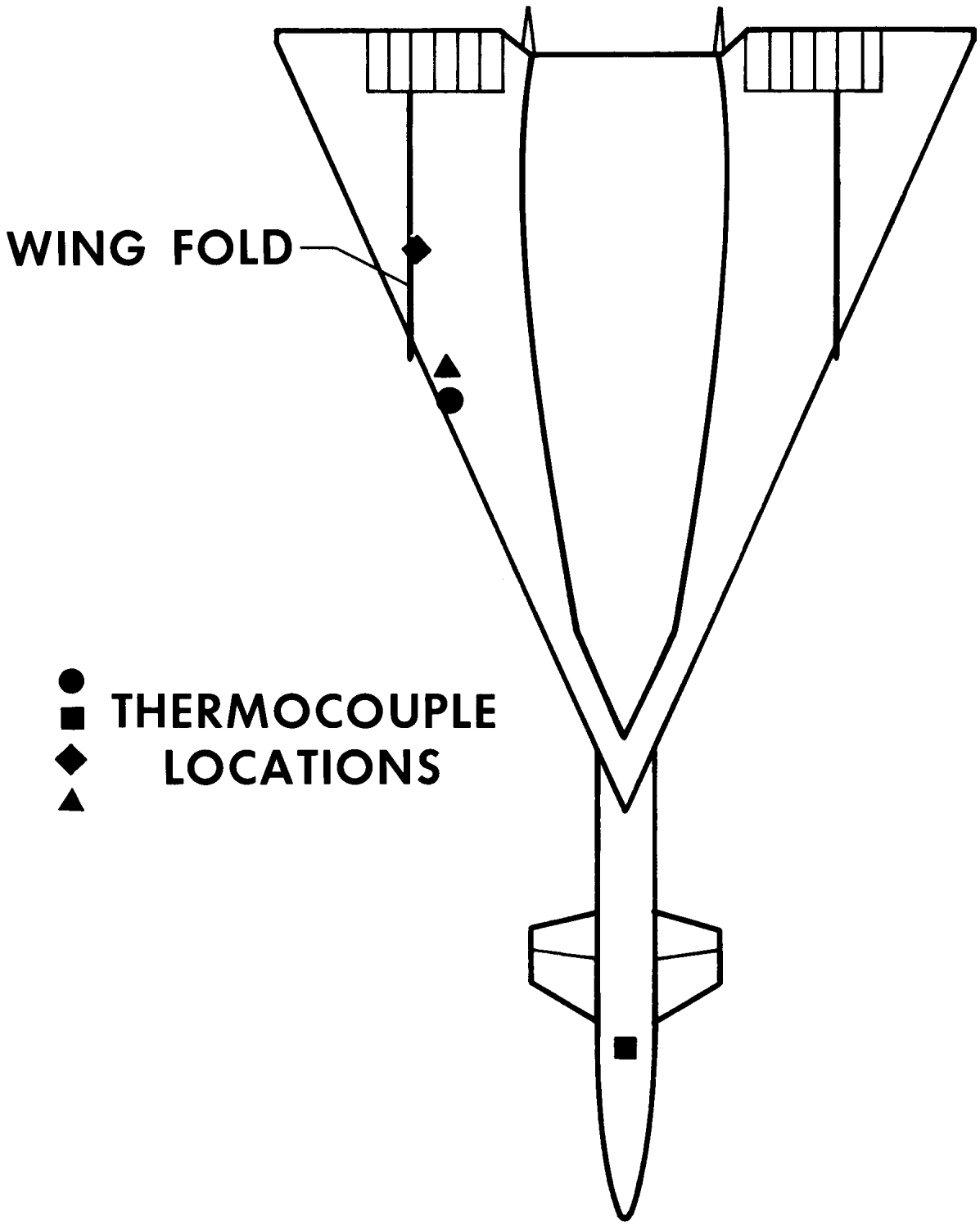

Figure 12. – Location of thermocouples used to demonstrate the variation in temperature gradients throughout the flight envelope.

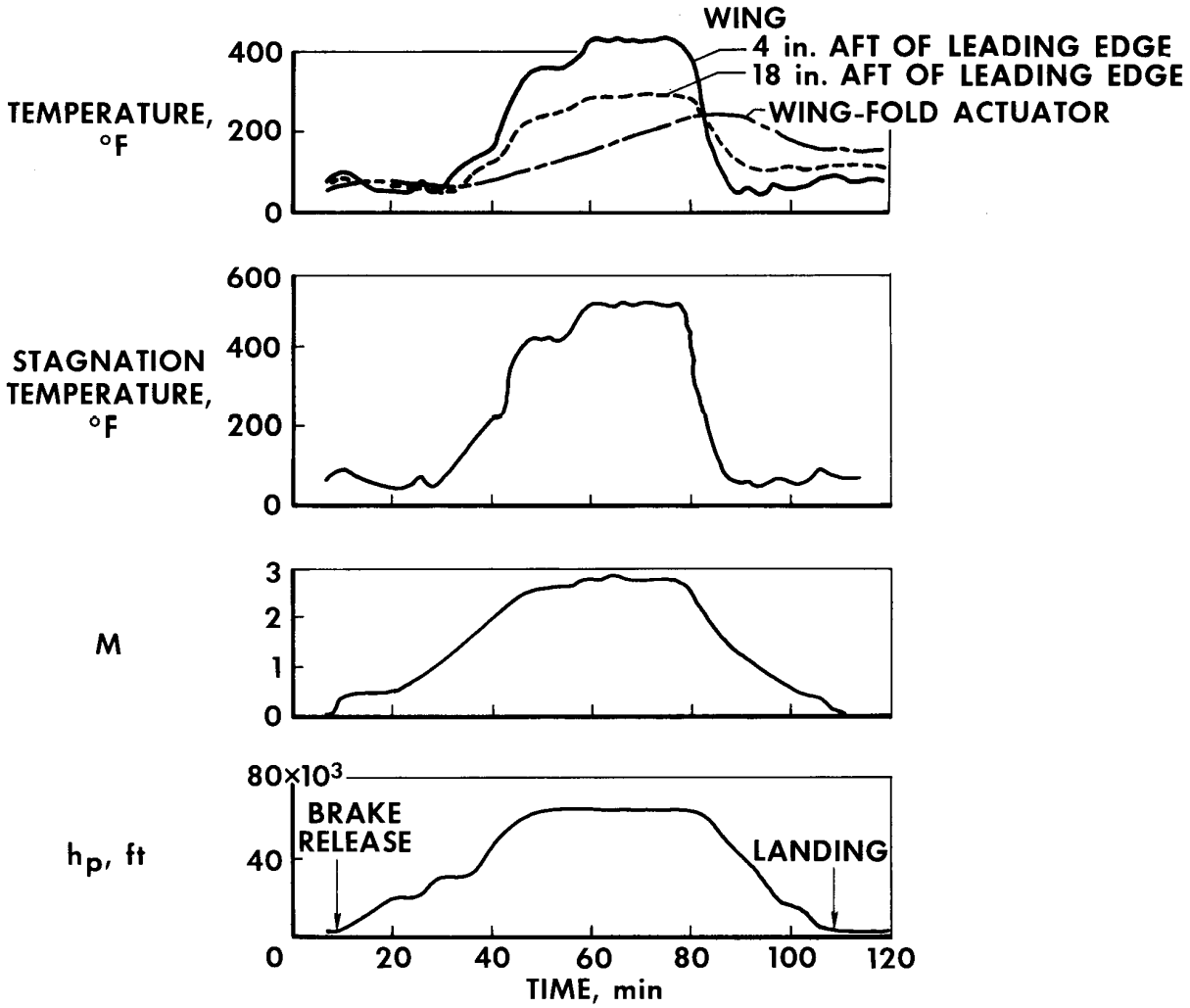

Figure 13. – Typical time history of temperature variations on the wing lower surface and wing-fold actuator.

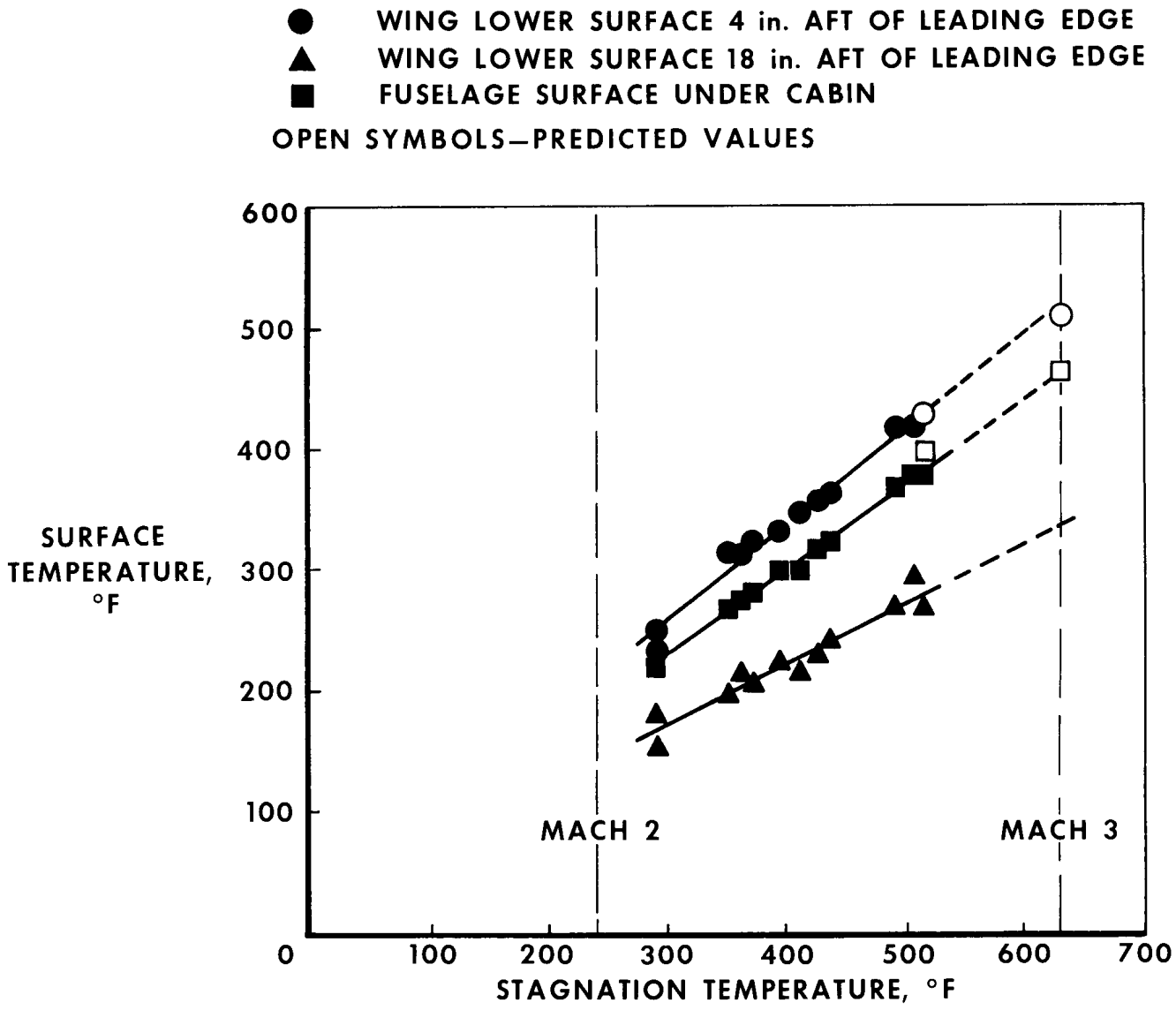

Figure 14. – Comparison of the lower-wing and forward-fuselage temperature gradients with theoretical predictions.

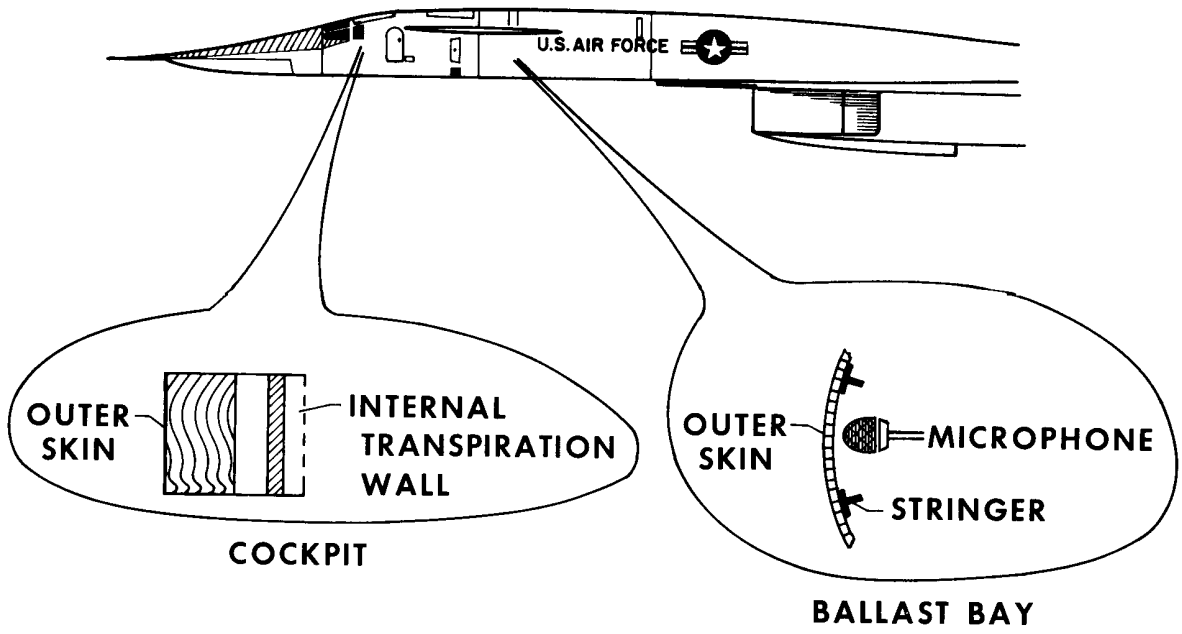

Figure 15. – Schematic illustration of internal acoustical instrumentation in the forward portion of the fuselage and associated fuselage wall construction.

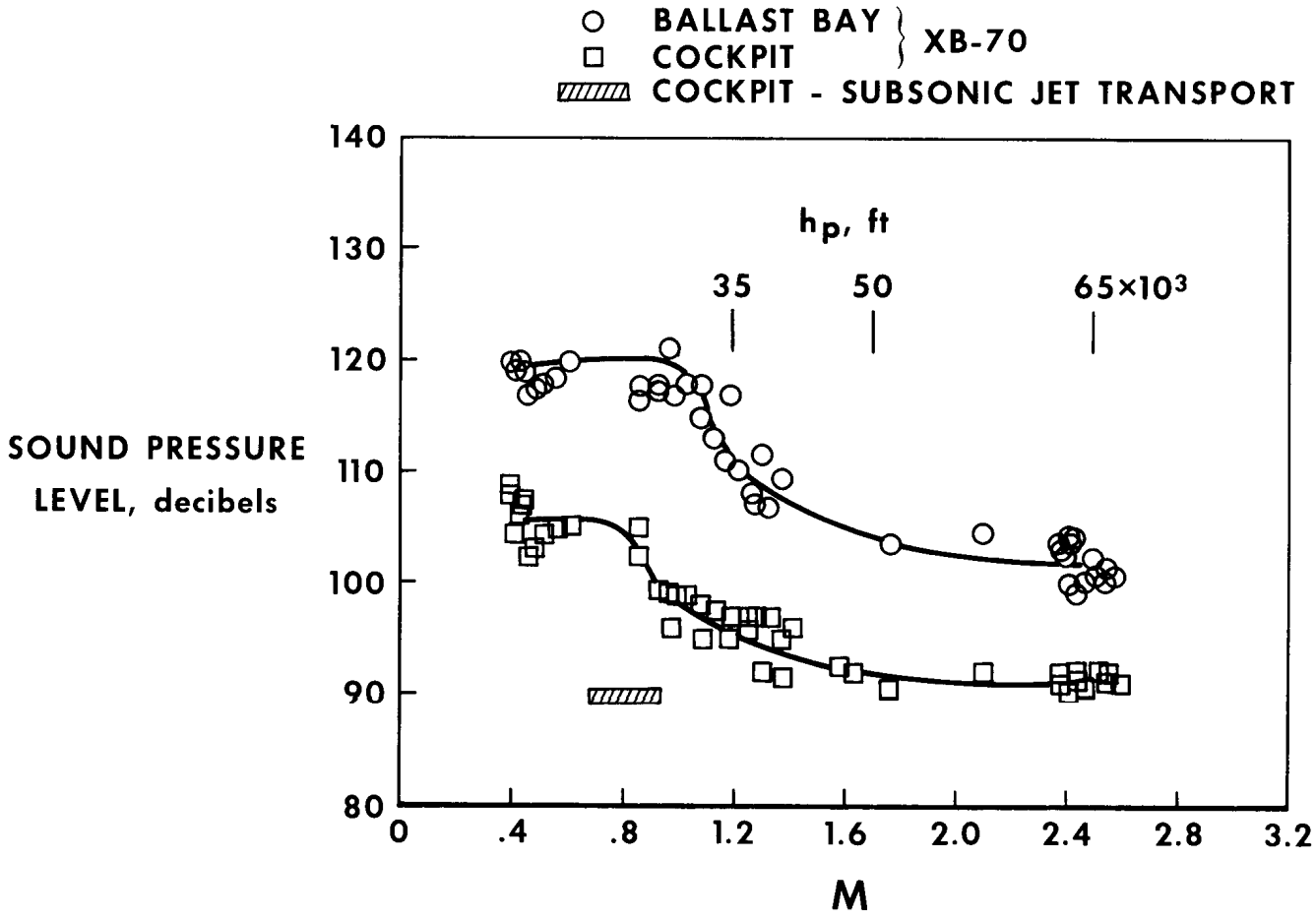

Figure 16. – Comparison of internal-noise measurements in the cockpit and ballast bay of the XB-70 forward fuselage with those measured in a subsonic jet transport.

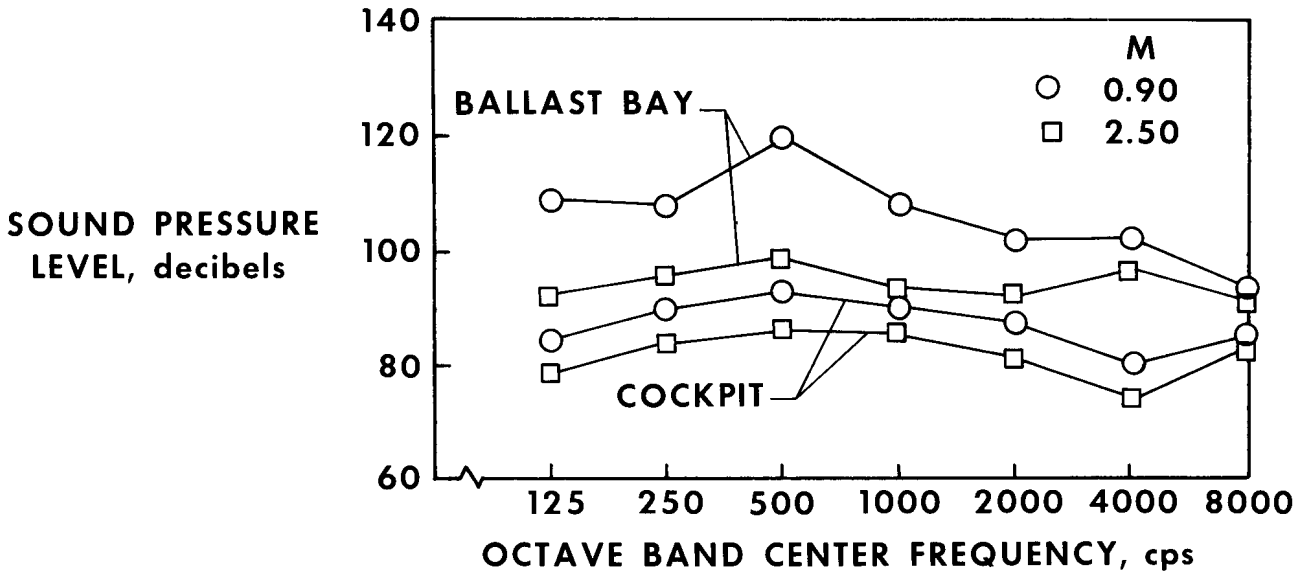

Figure 17. – Variation of the sound pressure spectrum with frequency measured in the cockpit and ballast bay at Mach numbers of 0.9 and 2.50.

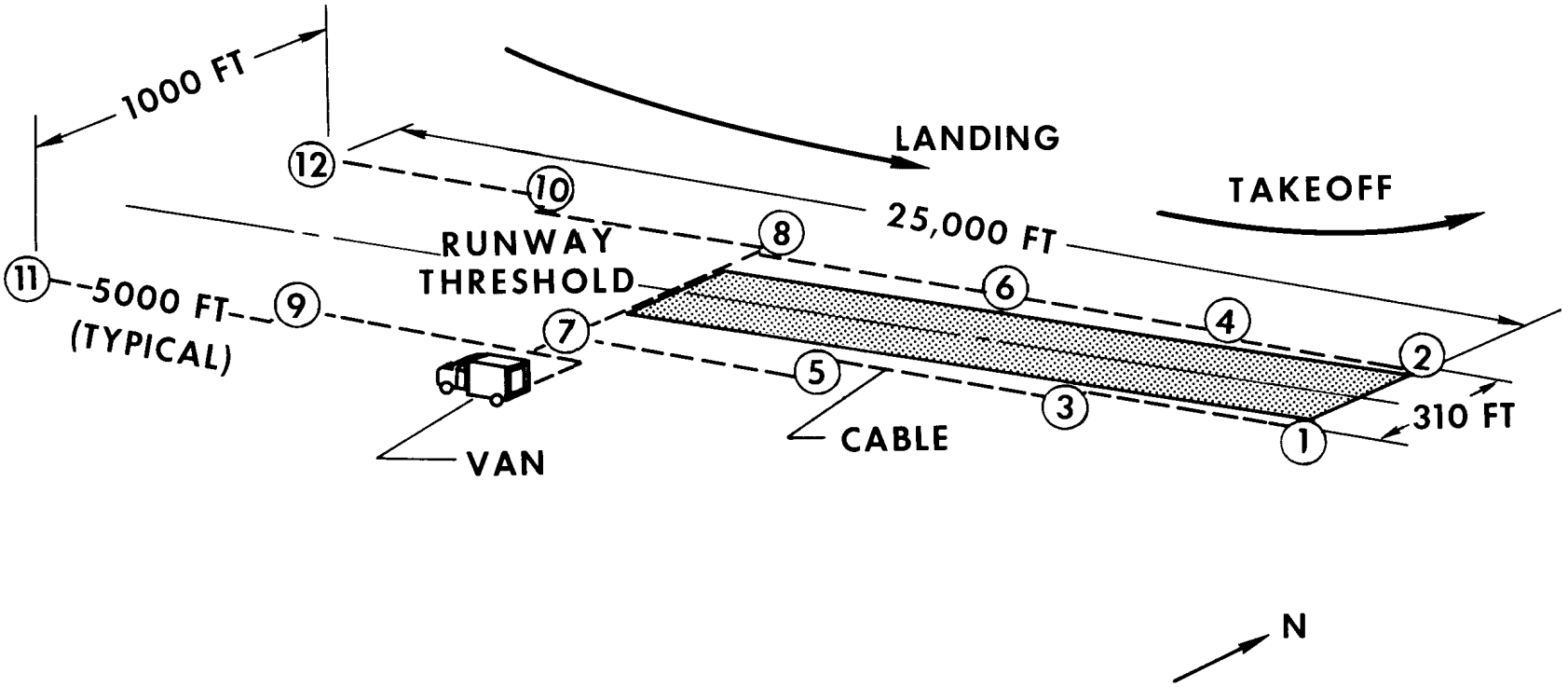

Figure 18. – Schematic of runway noise instrumentation installed along and beyond the west end of the runway at Edwards Air Force Base. Elevation = 2300 feet.

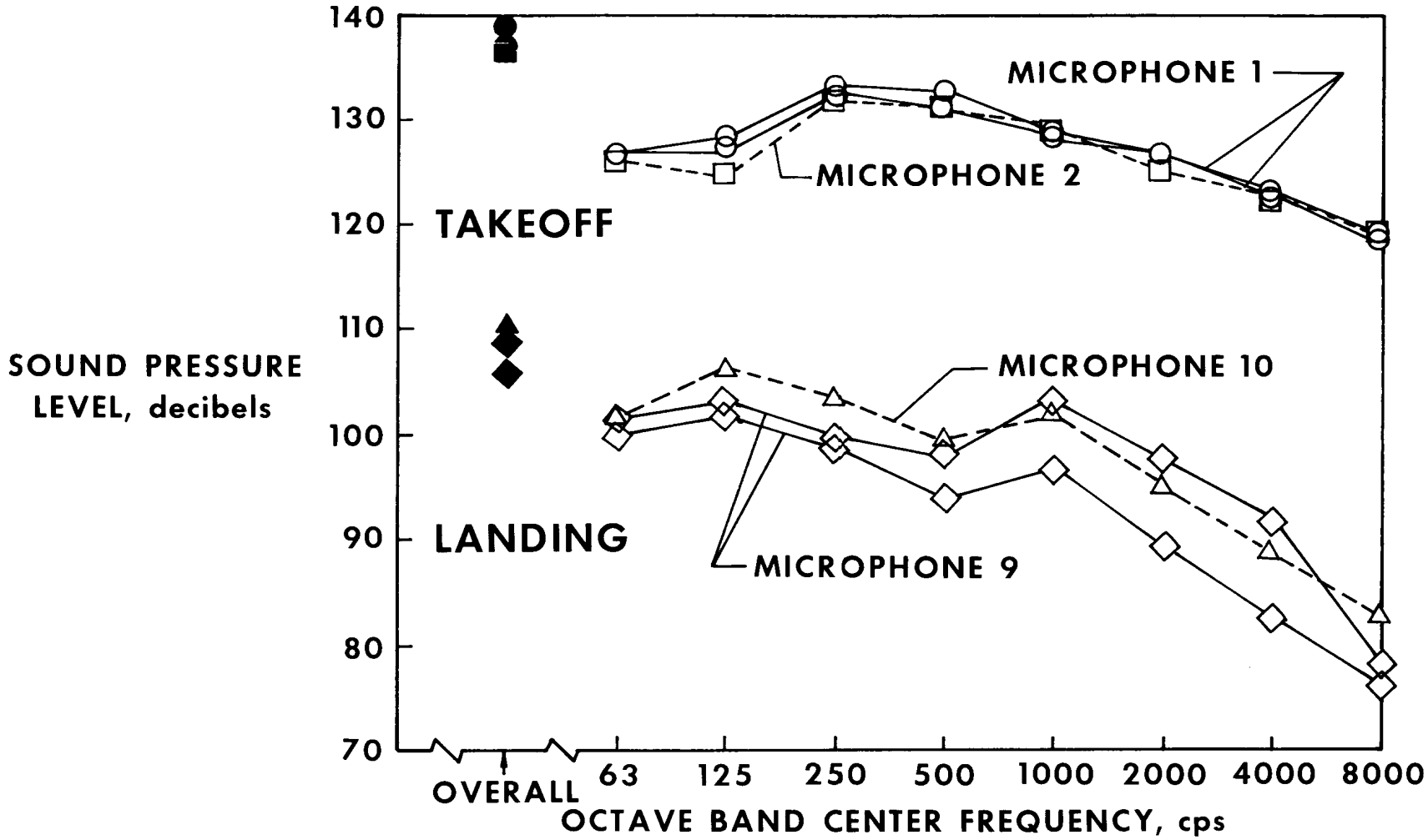

Figure 19. – Variation of sound pressure levels with frequency measured at four microphone stations during a typical XB-70 takeoff. Solid symbols denote average sound pressure levels.

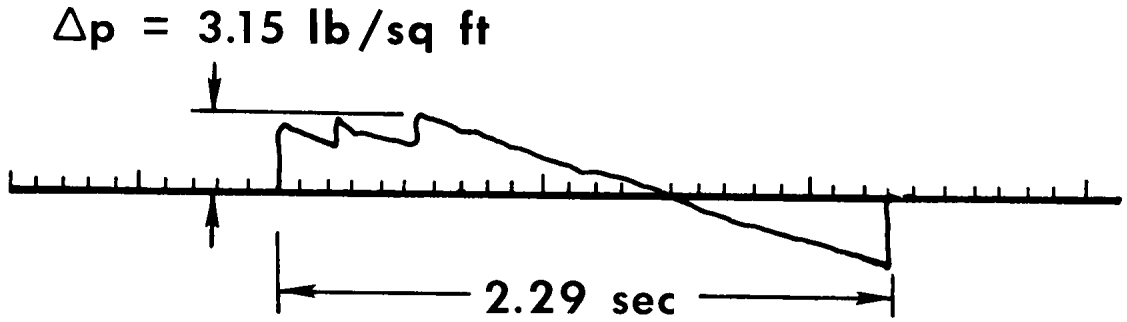

(a) M = 1.22, Δh = 27,000 ft, gross weight = 423,000 lb.

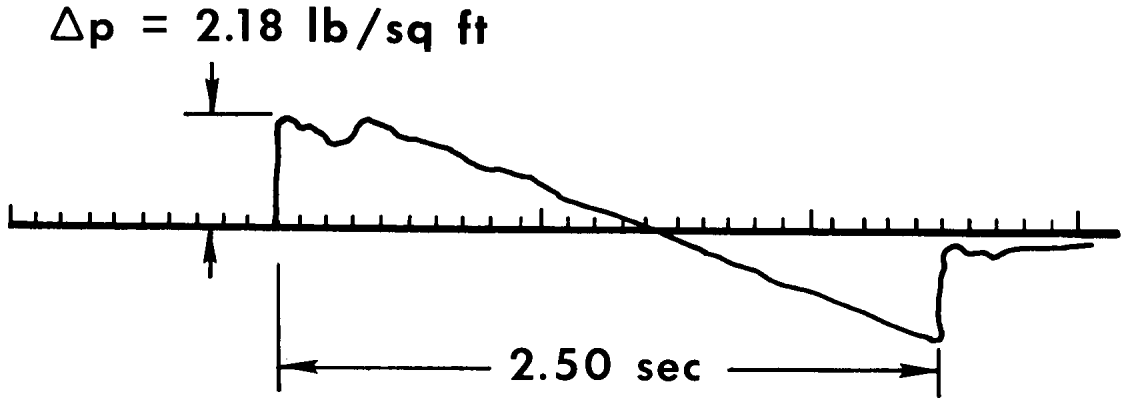

(b) M = 1.4, Δh = 38,700 ft, gross weight = 357,000 lb.

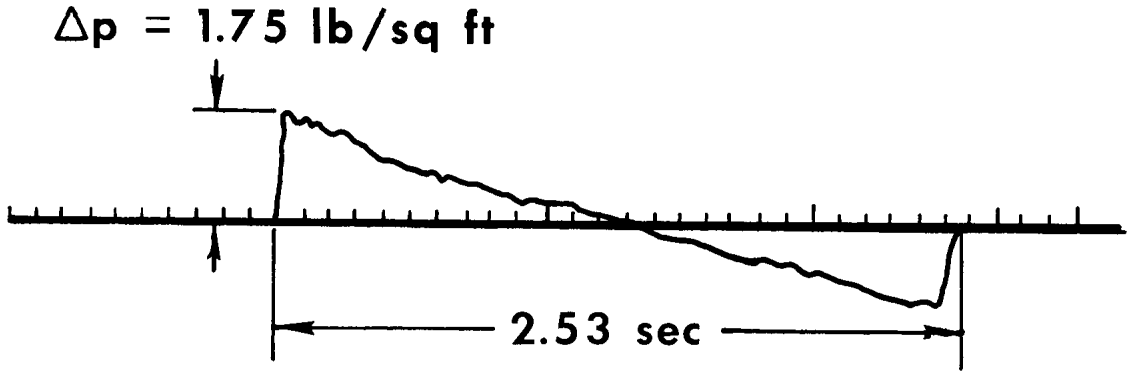

(c) M = 1.86, Δh = 48,000 ft, gross weight = 352,000 lb.

Figure 20.– Typical sonic-boom overpressure signatures measured in both the near and far field.

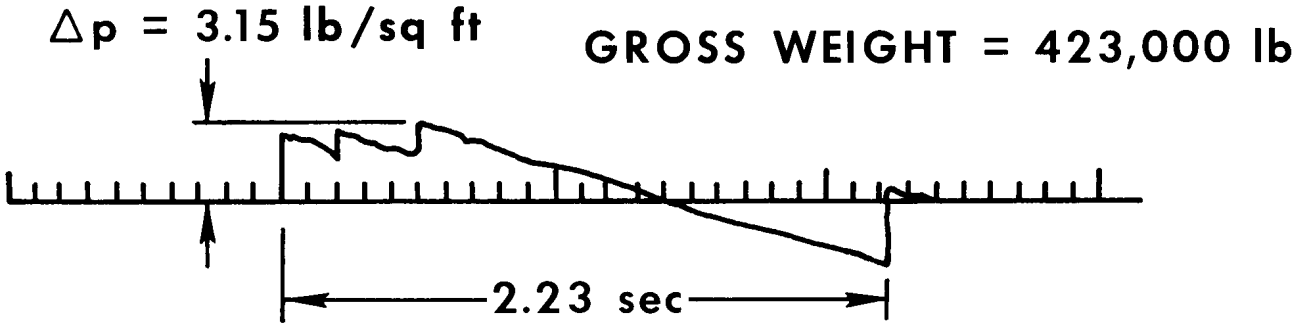

(a) XB-70 airplane.

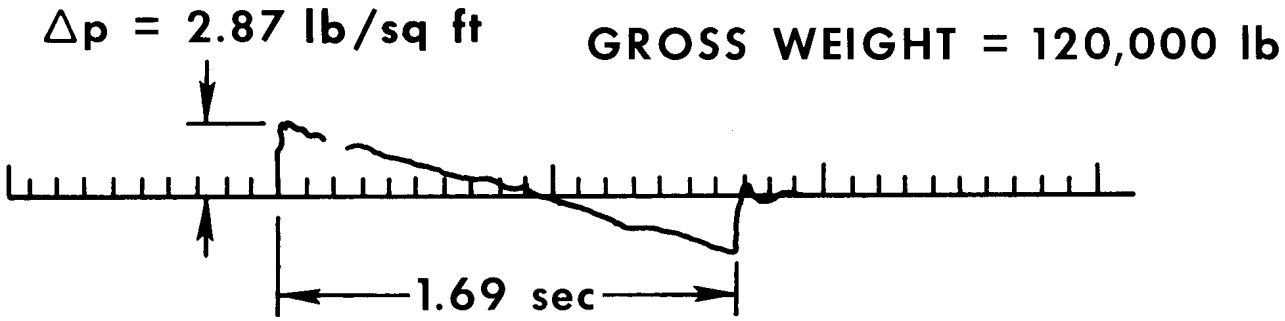

(b) B-58 airplane.

Figure 21. – Comparison of XB-70 and B-58 sonic-boom overpressure signatures measured in the near field of the XB-70. M = 1.22; Δh = 27,000 ft.